



Project *Life*-NEEVE:

Innovative technologies to monitor and reduce Non-Exhaust Emissions, particles and microplastics of VEHICLES and pavements to improve air quality and human health

LIFE-2023-SAP-ENV

(Circular Economy and Quality of LIFE-Standard Action Projects (SAP))



Deliverable D3.3:

**Innovative pavements for lower non-exhaust particle emissions**

Author(s):

Lorena Palomo Luis, CHM



### D3.3. Properties and design of road pavements with focus on non-exhaust particle emissions

Deliverable No.	D3.3
Deliverable Title	Innovative pavements for lower non-exhaust particle emissions
Dissemination	Public
Authors and partner acronyms	Lorena Palomo Luis, CHM V́ctor Garća Rabadán, CTCON Aida Domínguez-Sáez, CIEMAT Paloma Álvarez Mateos, US
Reviewed by	Mats Gustafsson, VTI Tawfiq Al Wasif-Ruiz, CIEMAT
Approved by	Paloma Álvarez Mateos, US
First version, date	Version 1, 2026-01-20
This version, date	Version 3, 2026-04-28



### D3.3. Properties and design of road pavements with focus on non-exhaust particle emissions

## SUMMARY

This deliverable presents the assessment and design of innovative asphalt pavement solutions within the LIFE NEEVE project, focusing on the relationship between asphalt mixture design, functional performance and non-exhaust emissions (NEE).

The work builds upon the methodological framework developed in Task 2.4 and is based on a controlled laboratory experimental programme aimed at characterising different asphalt mixtures in terms of mechanical behaviour, surface properties (texture and drainage capacity), and their influence on particle emissions. A dedicated experimental setup was implemented to reproduce tyre–pavement interaction under controlled conditions, enabling the analysis of particle emissions in terms of mass and size distribution.

Three pavement typologies were evaluated: SMA-11 (reference mixture), PA-11 (porous asphalt) and OSMA-11 (open-textured hybrid solution). The results highlight the strong influence of asphalt mixture design on both functional performance and emission-related behaviour. While PA is characterised by a highly open structure and more intense interaction processes, SMA provides a more compact and mechanically stable solution with lower overall emission levels. In this context, OSMA emerges as a balanced configuration, offering a compromise between surface functionality, mechanical performance and reduced emission potential.

Overall, the findings confirm that pavement surface characteristics, such as particularly texture, void structure and aggregate configuration, play a key role in particle generation, retention and resuspension processes. In this context, optimised and hybrid asphalt solutions such as OSMA show significant potential to reduce non-exhaust emissions while maintaining adequate mechanical and functional performance.

These results provide a solid basis for the identification and further validation of low-emission pavement solutions under real operating conditions, contributing to the development of more effective and sustainable road infrastructure strategies for reducing non-exhaust emissions.

## List of abbreviations and symbols

In this Deliverable abbreviations or symbols in the table below are often used.

Abbreviation	Explanation	Comment
<b>Partners, companies or institutions related to this project</b>		
CHM	CHM Obras e Infraestructuras S.A.	Partner
CTCON	Centro Tecnológico de la Construcción Región de Murcia	Partner
CIEMAT	Centro de Investigaciones Energéticas, Medioambientales y Tecnológicas	Partner
US	Universidad de Sevilla	Coordinator / Partner
VTI	Statens Väg- och Transportforskningsinstitut	Partner
<b>Technical terminology</b>		
NEE	Non-exhaust emissions	
PM	Particulate matter	
PM10	Particulate matter with aerodynamic diameter below 10 $\mu\text{m}$	
PM2.5	Particulate matter with aerodynamic diameter below 2.5 $\mu\text{m}$	
PN	Particle number	
TRWP	Tyre and road wear particles	
SMA	Stone Mastic Asphalt	
PA	Porous Asphalt	
OSMA	Open-textured Stone Mastic Asphalt	
PMB	Polymer-modified bitumen	
RTFOT	Rolling Thin Film Oven Test	
LA	Los Angeles coefficient	
PSV	Polished Stone Value	
MTD	Mean Texture Depth	
PTV	Pendulum Test Value	
WTS	Wheel Tracking Slope	
BSL	Baseline mixture	
SP	Steel particles	
OPS	Optical Particle Sizer	
LPI	Low Pressure Impactor	
<b>Measures and units</b>		
Mm	Milimeters	
$\mu\text{m}$	Micrometers	
nm	Nanometers	
g	Grams	
mg	Miligrams	
ml	Mililiters	
s	Seconds	
min	Minutes	



### D3.3. Properties and design of road pavements with focus on non-exhaust particle emissions

Abbreviation	Explanation	Comment
h	Hours	
°C	Degrees Celsius	
MPa	Megapascals	
mPa.s	Milipascals seconds	
L/min	Litres per minute	
km/h	Kilometres per hour	
mm/1000 cycles	Wheel tracking slope /rutting rate	



## Table of contents

<b>1. INTRODUCTION</b> .....	<b>1</b>
<b>2. PURPOSE AND OBJECTIVE</b> .....	<b>3</b>
<b>3. METHODOLOGICAL FRAMEWORK</b> .....	<b>4</b>
<b>3.1 Overall experimental design</b> .....	<b>4</b>
3.1.1. Aggregates characterisation.....	4
3.1.2. Asphalt sample characterisation .....	5
3.1.3. NEE from asphalt perspective.....	10
<b>3.2 Coordination between CHM, VTI, CIEMAT, CTCON, US</b> .....	<b>14</b>
<b>4. MATERIALS</b> .....	<b>15</b>
<b>4.1 Aggregates</b> .....	<b>15</b>
4.1.1. Description of aggregate types.....	15
4.1.2. Mechanical characterisation of aggregates .....	17
4.1.3. Chemical and mineralogical characterisation (XRD) .....	18
<b>4.2 Bitumen</b> .....	<b>19</b>
<b>4.3 Steel Materials</b> .....	<b>20</b>
<b>5. DESCRIPTION OF ASPHALT MIXTURES PRODUCES</b> .....	<b>23</b>
<b>5.1 Laboratory production procedures</b> .....	<b>23</b>
<b>5.2 Reference pavement (SMA 11)</b> .....	<b>24</b>
5.2.1. Porphyritic coarse fraction 5/11.....	24
5.2.2. Porphyritic coarse fraction 6/12.....	25
<b>5.3 Open graded SMA 11 (hybrid solution)</b> .....	<b>27</b>
5.3.1. Porphyritic coarse fraction 5/11 .....	27
5.3.2. Porphyritic coarse fraction 6/12.....	28
<b>5.4 Porous asphalt pavement (PA 11)</b> .....	<b>30</b>
5.4.1. Porphyritic coarse fraction 5/11 .....	30



**D3.3. Properties and design of road pavements with focus on non-exhaust particle emissions**

5.4.2. Porphyritic coarse fraction 6/12.....	31
<b>5.5 Additional pavement types evaluated .....</b>	<b>33</b>
<b>6. RESULTS .....</b>	<b>34</b>
<b>6.1 Asphalt characterisation .....</b>	<b>34</b>
6.1.1. Mechanical performance.....	34
6.1.2. Particle loss analysis.....	35
6.1.3. Texture analysis.....	38
6.1.4. Drainage capacity .....	40
<b>6.2 NEE Physical Characterisation .....</b>	<b>41</b>
<b>7. RISKS, LIMITATIONS AND LESSONS LEARNED .....</b>	<b>47</b>
<b>8. CONCLUSIONS.....</b>	<b>48</b>
<b>9. ACKNOWLEDGMENTS .....</b>	<b>50</b>
<b>10. REFERENCES.....</b>	<b>51</b>





### D3.3. Properties and design of road pavements with focus on non-exhaust particle emissions

## 1. Introduction

Air pollution continues to represent a major environmental and public health challenge, particularly in urban areas where road transport is one of the main contributing sources. In recent decades, regulatory frameworks and technological advancements have led to a significant reduction in exhaust emissions from vehicles. However, non-exhaust emissions (NEE) have emerged as an increasingly relevant and still largely unregulated source of particulate matter (PM), including particles generated from tyre wear, brake wear, and road surface interaction. Current projections indicate that NEE will dominate traffic-related PM emissions in the coming years (European Environment Agency, 2020).

Among the different sources of NEE, the interaction between tyres and pavement surfaces plays a major role in both the generation and resuspension of particulate matter. The mechanical processes occurring at the tyre–pavement interface, including friction and abrasion, lead to the release of particles originating from both materials, forming complex mixtures commonly referred to as tyre and road wear particles (TRWP). These particles cover a wide size range, from coarse fragments to fine and ultrafine particles (PM<sub>10</sub> and PM<sub>2.5</sub>) and may contain mineral components, polymers, and potentially harmful substances. As a result, the design and properties of the pavement surface have a direct influence on the quantity, characteristics, and behaviour of emitted particles.

Pavement characteristics such as aggregate type, gradation, surface texture, and mechanical resistance are particularly relevant in this context. Surface macrotexture and microtexture influence tyre wear mechanisms and frictional behaviour, while also affecting the retention and resuspension of road dust. Additionally, the use of wear-resistant aggregates and optimised mixture designs has been identified as a potential strategy to reduce particle generation and improve the overall environmental performance of road pavements (Gehrke et al., 2023).

In response to this challenge, the LIFE NEEVE project aims to develop, validate, and demonstrate innovative solutions for the measurement and reduction of non-exhaust emissions from road transport. The project adopts an integrated approach, addressing both vehicle-related components and road infrastructure, with a particular focus on improving the interaction between tyres and pavement surfaces. Within this framework, the design of advanced asphalt mixtures is identified as a key strategy to minimise particle generation and mitigate NEE.

The present deliverable builds upon the work carried out in Task 2.4, where a comprehensive methodology was developed to assess the influence of asphalt pavement design on NEE. This work combined a state-of-the-art review with an extensive experimental programme, enabling the characterisation of different asphalt mixtures in terms of mechanical performance, surface properties, and their potential impact on particle emissions. The results obtained provided a robust technical basis for the identification of promising pavement solutions, including hybrid configurations that balance durability, surface functionality, and emission-related performance.



### **D3.3. Properties and design of road pavements with focus on non-exhaust particle emissions**

In this context, this deliverable aims to assess the performance of the selected asphalt mixtures in terms of their potential influence on non-exhaust emissions. The analysis builds upon the experimental and methodological framework defined in Task 2.4, enabling a consistent evaluation of the relationship between pavement design parameters and particle generation mechanisms. In doing so, it contributes to the overall assessment of the proposed solutions within the LIFE NEEVE project framework.

Furthermore, the analysis presented in this deliverable is intended to provide a deeper understanding of the mechanisms governing particle generation and release at the pavement surface, considering both material-related properties and functional performance parameters. By linking mixture design characteristics with emission-related behaviour, this work contributes to advancing the knowledge required for the development of more effective and environmentally optimised pavement solutions, while supporting their future validation under real operating conditions.



### D3.3. Properties and design of road pavements with focus on non-exhaust particle emissions

## 2. Purpose and Objective

The main objective of this deliverable is to assess the performance of the selected asphalt pavement solutions in terms of their influence on particle generation and release mechanism associated with non-exhaust emissions (NEE), with particular focus on the tyre-pavement interaction. In this context, this task aims to further advance the understanding of how pavement design parameters influence the generation, release and potential resuspension of particulate matter, contributing to the development of more environmentally optimised road surfaces.

Building upon the methodology and results developed in Task 2.4, this deliverable focuses on the analysis and design of asphalt mixture solutions, ensuring consistency in the evaluation approach. This work extends the assessment from material design and laboratory characterisation towards a more emission-oriented perspective, linking mechanical and functional properties with their potential environmental impact.

All things considered, the specific objectives of this deliverable are detailed as follows:

- To analyse the behaviour of selected asphalt mixtures in relation to particle generation mechanisms associated with tyre–pavement interaction.
- To assess the influence of key pavement parameters, such as aggregate gradation, surface texture, and mechanical performance, on non-exhaust emissions.
- To evaluate the potential of innovative asphalt mixtures to reduce particle emissions compared to conventional pavement solutions.
- To contribute to the identification of pavement configurations with improved environmental performance, supporting their selection for further validation stages within the project.

Overall, this deliverable expects to contribute to the ongoing development and assessment of low-emission pavement solutions within the LIFE NEEVE project, supporting the transition from laboratory-scale analysis to subsequent validation under real operating conditions.



## 3. Methodological Framework

### 3.1 Overall experimental design

#### 3.1.1. *Aggregates characterisation*

The laboratory testing campaign carried out within the Life NEEVE project includes an initial phase focused on the characterisation of the coarse aggregate materials considered to produce the different asphalt mixture hypothesis. This step is essential to verify the compliance of the selected materials with the European standards and to assess their suitability in terms of mechanical performance and durability.

The importance of aggregate properties in asphalt mixtures is directly related to their impact on performance, as geometrical, mechanical, and surface characteristics govern stability, durability, and skid resistance. From a NEE perspective, these properties are especially critical, since degradation mechanisms such as fragmentation and polishing may contribute to the generation of non-exhaust particulate matter.

To this end, a comprehensive laboratory testing programme was conducted to evaluate the key properties of the aggregate, particularly those related to mechanical degradation processes linked to non-exhaust emissions. These tests are presented as follows.

- **Particle size distribution**

The particle size distribution of the aggregates was determined by using the sieving method, in accordance with UNE-EN 933-1. This test allows the classification of aggregates according to their granulometry, which is a key parameter in the design of asphalt mixtures.

This procedure consists of passing a representative sample through a series of standardized sieves with decreasing mesh sizes, determining the percentage of material retained on each sieve. The resulting grading curve is used to verify compliance with the specified limits and to ensure an appropriate particle size distribution for mixture design.

A proper granulometric distribution is essential to achieve adequate compaction, interlocking between particles, and a suitable void structure, all of which directly influence the mechanical performance and durability of the asphalt mixture.

- **Resistance to fragmentation – Los Angeles abrasion test**

The resistance to fragmentation of the aggregates was determined using the Los Angeles (LA) test, in accordance with UNE-EN 1097-2. This test evaluates the ability of aggregates to withstand mechanical degradation due to impact and abrasion.

The test consists of placing a defined quantity of aggregate together with steel balls inside a rotating drum. After a specified number of revolutions, the material is sieved, and the percentage of generated fines is calculated as the Los Angeles coefficient.

### D3.3. Properties and design of road pavements with focus on non-exhaust particle emissions

Lower LA values indicate higher resistance to fragmentation and, consequently, a reduced susceptibility to mechanical degradation. This aspect is particularly critical in the context of non-exhaust emissions, as aggregates with poor resistance are more prone to generate fine particles due to impact and abrasion processes, contributing significantly to particulate matter emissions.

- **Polished Stone Value – PSV**

The resistance of aggregates to polishing was evaluated by means of the Polished Stone Value (PSV), in accordance with UNE-EN 1097-8. This test, as shown in Figure 1, assesses the susceptibility of aggregates to surface polishing under traffic action, which is directly related to the skid resistance of the pavement.

This procedure consists of subjecting aggregate samples to an accelerated polishing process using a standardized procedure that simulates the mechanical action of traffic. After polishing, the frictional properties of the aggregate surface are measured using a pendulum tester, providing an index value representative of the retained microtexture.



Figure 1. Overview of PSV testing device

From a design perspective, the selection of the appropriate PSV level requires a balanced approach. While high PSV values are traditionally associated with improved skid resistance due to better microtexture retention, they may also contribute to increased tyre wear as a result of higher friction at the tyre–pavement interface. In the context of the Life NEEVE project, this aspect is particularly relevant, as tyre wear is a major source of non-exhaust particulate emissions.

#### 3.1.2. Asphalt sample characterisation

Following the characterization of the aggregates, a comprehensive laboratory testing programme was carried out on asphalt mixtures in order to evaluate their mechanical performance and functional properties. These tests were selected in accordance with relevant standards and aimed at assessing the behaviour of the mixtures under conditions representative of in-service pavement performance.

### D3.3. Properties and design of road pavements with focus on non-exhaust particle emissions

The evaluated properties include stiffness, resistance to permanent deformation, particle loss due to mechanical action, skid resistance, and drainage capacity, in line with the methodology defined in Deliverable D2.4, where the key properties and corresponding test methods for assessing NEE-related performance were established.

All things considered, the main test performed for the characterisation of the asphalt mixtures are described as follows:

- **Stiffness resistance**

The stiffness of the asphalt mixtures, in accordance with UNE-EN 12697-26, was evaluated in order to characterise their mechanical response under traffic loading conditions (see Figure 2). This property reflects the ability of the material to distribute stresses and resist deformation, and it is therefore a key parameter in pavement design and performance assessment.

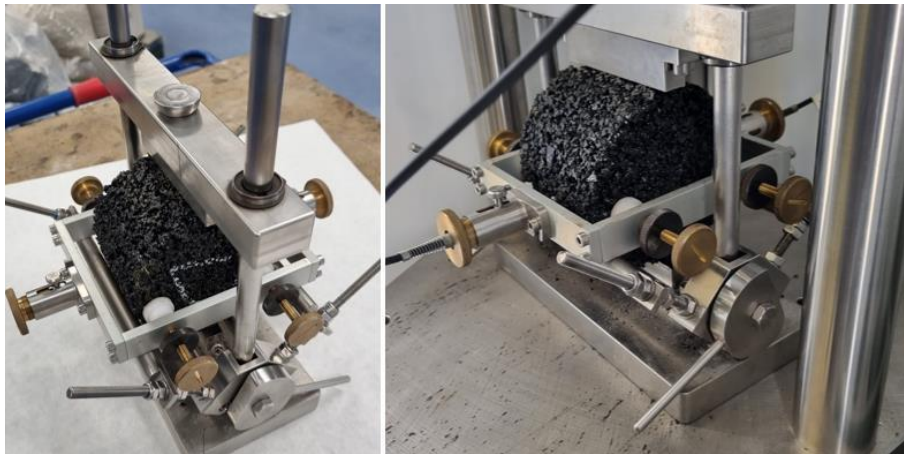


Figure 2. Overview stiffness testing procedure

The test consists of applying a cyclic load to a prepared asphalt specimen while measuring the resulting deformation, allowing the calculation of the stiffness modulus as an indicator of the material's resistance to deformation under repeated traffic loads. This parameter is closely related to both structural performance and durability, as mixtures with inadequate stiffness may be more susceptible to deformation or cracking, potentially accelerating surface degradation processes. In the context of non-exhaust emissions, this aspect is particularly relevant, since pavement deterioration can contribute to the generation of particulate matter.

- **Resistance to permanent deformation – Wheel tracking test**

The resistance of asphalt mixtures to permanent deformation was evaluated using the wheel tracking test, in accordance with UNE-EN 12697-22, as shown in Figure 3. This test assesses the susceptibility of the material to rutting under repeated traffic loading, which is a key parameter for the long-term performance of pavements.

The test consists of subjecting a slab specimen to repeated passes of a loaded wheel under controlled temperature conditions (at 60°C), simulating the effect of traffic loads over time. In this case, the test was carried out up to 10,000 load cycles, during which the progressive accumulation of deformation was continuously measured, allowing the determination of parameters such as rut depth and deformation rate.

### D3.3. Properties and design of road pavements with focus on non-exhaust particle emissions

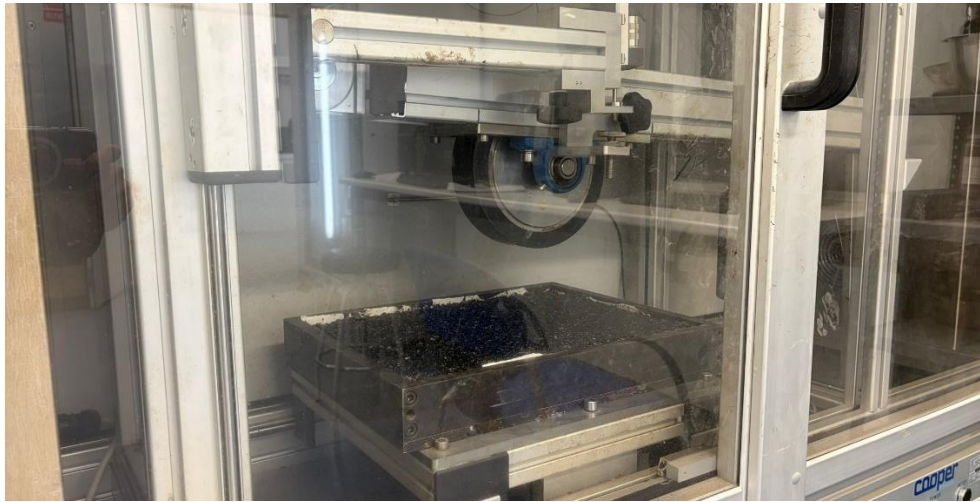


Figure 3. Overview wheel tracking test procedure

The resistance to permanent deformation is directly related to the stability and durability of the mixture, as materials with poor performance are more prone to rutting and surface deterioration. In the context of non-exhaust emissions, this behaviour is particularly relevant, since the development of ruts can enhance surface wear mechanisms and contribute to the generation and accumulation of particulate matter.

- **Particle loss analysis (Cantabro test)**

The resistance of asphalt mixtures to particle loss was evaluated using the Cantabro test, in accordance with UNE-EN 12697-17. This test assesses the cohesion of the mixture and its susceptibility to ravelling, by quantifying the mass loss of a compacted specimen subjected to mechanical action (see Figure 4).

This parameter is especially relevant in the context of non-exhaust emissions, as it directly quantifies the tendency of the mixture to release particles due to traffic-induced stresses. Asphalt mixtures with high particle loss values are more prone to surface degradation and ravelling, contributing to the generation of particulate matter.



Figure 4. Appearance of asphalt samples after Cantabro test (extracted from D2.4)

### D3.3. Properties and design of road pavements with focus on non-exhaust particle emissions

- **Prall test**

At VTI, Marshall samples, prepared at CTCON of six material and construction combinations was tested for abrasion resistance using the Prall method (SS-EN 12697-16:2016). The samples were SMA11, OSMA11 and PA11, all made with two gradings of porphyry, 5/11 and 6/12.

The Prall test simulates abrasion resistance of the sample surface and is mainly used to investigate the resistance against wear from studded tyres in the Nordic countries. Briefly, the sample is oscillating and abraded by steel balls under a cooling water flow (Figure 5).

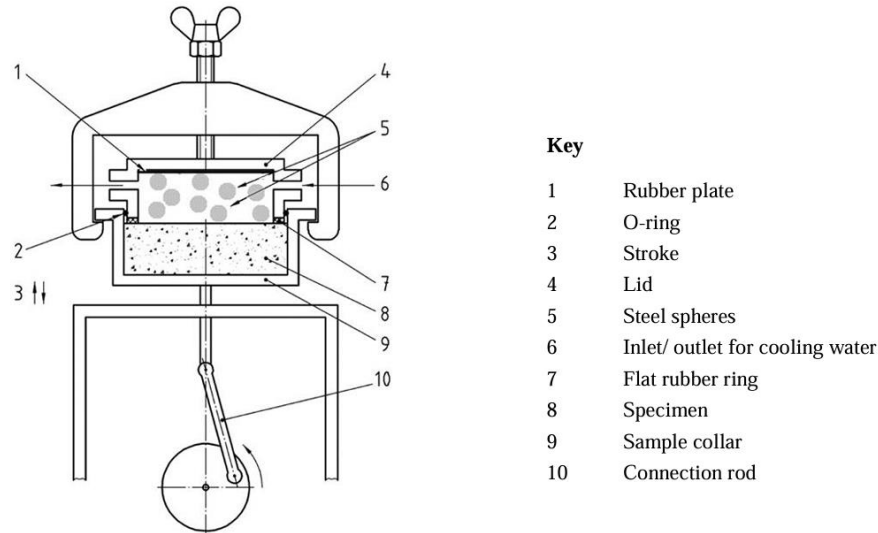


Figure 5. Overview of Prall apparatus (from Siebert & Mork, 2016)

- **Asphalt texture analysis**

The surface texture of asphalt mixtures, considering both macrotexture and microtexture, was analysed to evaluate its influence on tyre–pavement interaction and overall functional performance. Within the context of the LIFE NEEVE project, these properties are particularly relevant, as they directly affect not only friction performance but also tyre wear mechanisms, which are a major source of non-exhaust particulate emissions.

On one hand, the macrotexture of the asphalt mixtures was evaluated using the sand patch method, in accordance with UNE-EN 13036-1. This test determines the Mean Texture Depth (MTD) by measuring the area covered by a known volume of calibrated sand spread over the surface of the asphalt sample.

On the other hand, the microtexture of the asphalt mixtures was assessed through the pendulum test (see Figure 6), in accordance with UNE-EN 13036-4. This test provides an indirect measurement of surface friction by determining the energy loss of a rubber slider passing over the specimen, expressed as the Pendulum Test Value (PTV).

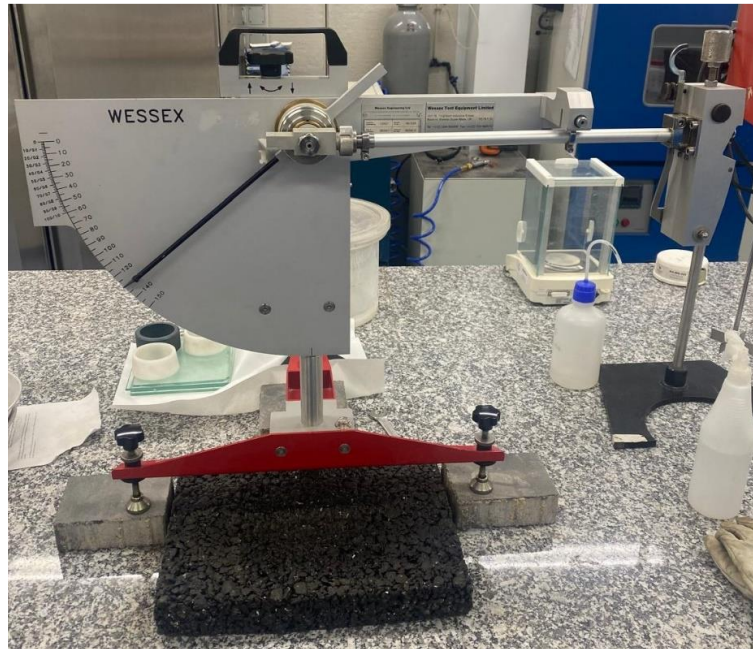


Figure 6. Overview pendulum test

- Drainability

The drainage capacity of the asphalt mixtures was evaluated in order to assess their ability to evacuate water through the surface, which is a key functional property for porous and semi-porous pavements. This test, as shown in Figure 7, was carried out in accordance with UNE-EN 12697-40 by measuring the flow of water through the asphalt specimen under controlled conditions, providing an indicator of the permeability of the mixture.

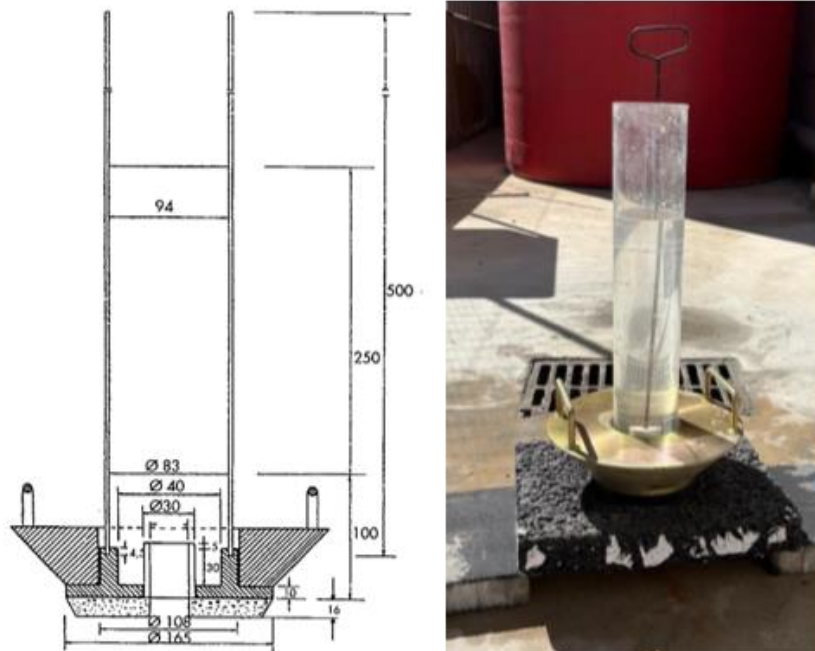


Figure 7. Overview asphalt drainage capacity



### D3.3. Properties and design of road pavements with focus on non-exhaust particle emissions

This property is particularly relevant for open-graded asphalt mixtures, as efficient water drainage contributes to reducing the accumulation of fine particles on the pavement surface. By limiting the presence of loose material and surface moisture, adequate drainage conditions may help to reduce particle resuspension under traffic action, thereby contributing to the mitigation of non-exhaust particulate emissions.

#### *3.1.3. NEE from asphalt perspective*

Understanding particle emissions generated by tyre/pavement interaction requires a controlled experimental approach capable of isolating the contribution of pavement properties from other influencing factors (as operating conditions, environmental variables, or tyre characteristics). In this context, a dedicated laboratory methodology, to the best of the authors' knowledge not previously applied to this specific problem, has been developed to reproduce tyre/pavement contact under well-defined and repeatable conditions, while enabling simultaneous characterization of the generated particles.

The experimental setup combines a mechanically controlled pavement loading system with a high-flow aerosol sampling line. This integrated configuration allows precise control of the contact conditions at the tyre/pavement interface and, at the same time, continuous measurement of particle emissions in terms of number, size distribution, and mass.

Friction is generated by advancing a replaceable pavement sample toward the rotating tyre using a mechanically actuated pressure jack. The pavement specimen is mounted on a rigid support structure incorporating hinged elements that ensure stable alignment and controlled positioning relative to the tyre tread. The displacement induced by the pressure jack progressively increases the normal force at the interface, promoting controlled wear and particle generation. The applied load is continuously monitored by an in-line load cell installed between the jack and the pavement support structure, enabling real-time measurement and fine adjustment of the contact force. This configuration is intended to ensure the highest possible level of reproducibility within the constraints of the available resources, providing stable and controlled tyre/pavement interaction throughout the test duration.

### D3.3. Properties and design of road pavements with focus on non-exhaust particle emissions

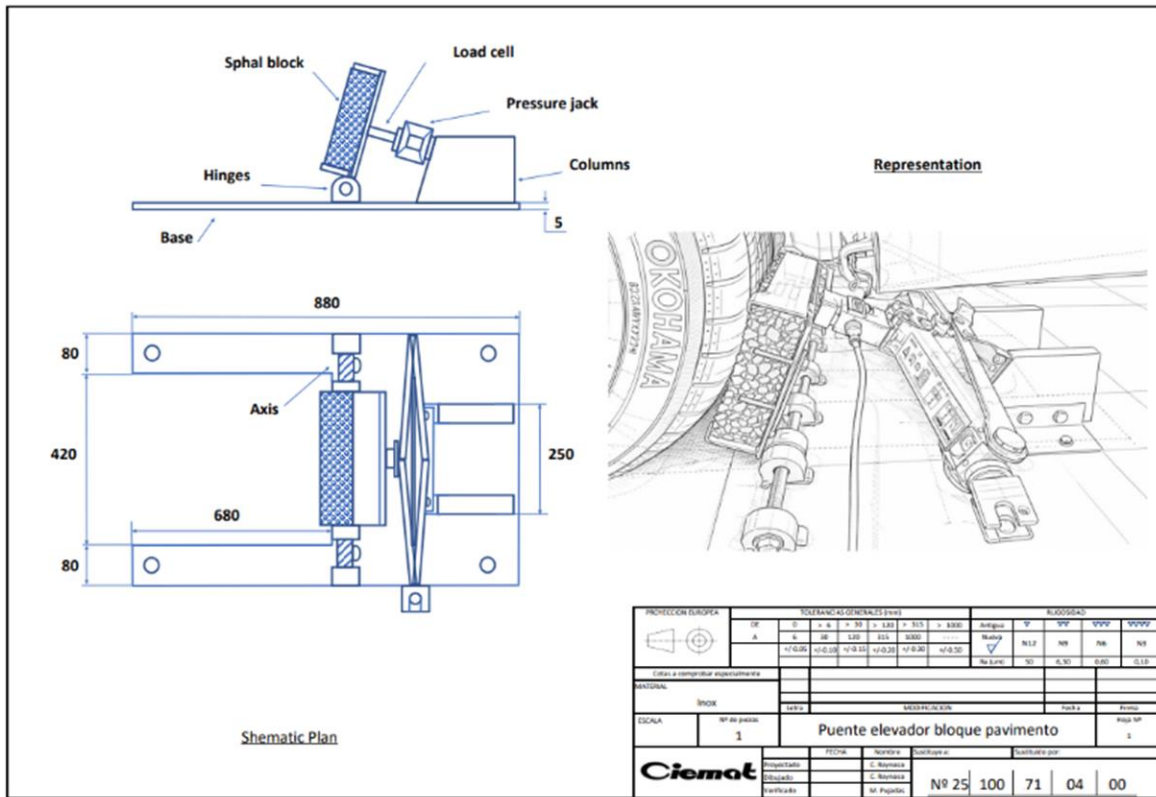


Figure 8. Overview of the mechanically controlled tyre-pavement loading system

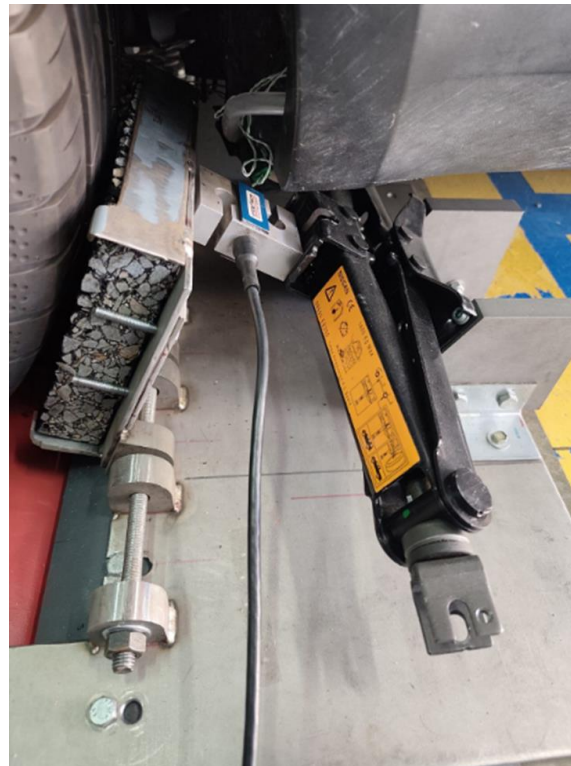


Figure 9. Detail of the pavement specimen holder and load application assembly

### D3.3. Properties and design of road pavements with focus on non-exhaust particle emissions

The particles generated at the contact interface are captured downstream of the tyre using a custom-designed sampling nozzle positioned close to the emission source. The nozzle directs the particle-laden airflow into a cylindrical main duct (internal diameter approximately 102 mm), where the aerosol is transported under high-flow suction conditions. A straight duct section of 950 mm was maintained upstream of the sampling ports to promote a more stable flow field before particle extraction. The primary airflow, maintained at approximately 5400 L/min by an industrial vacuum cleaner (Nilfisk GS 83) supported by an auxiliary vacuum pump, promotes particle transport towards the sampling line, although some deposition losses cannot be fully excluded.

A controlled sub-sampling branch is extracted from the main duct to measure particle number concentration and size distribution in real time. This branch supplies an OBS ONE-PN10 instrument and an Optical Particle Sizer (OPS), operating at low flow rates (approximately 0.7 L/min and 1.0 L/min, respectively). In parallel, an eleven-stage Low Pressure Cascade Impactor (Hauke LPI25) operating at 25 L/min enables size-segregated particle collection for subsequent gravimetric mass determination. The sub-sampling inlet was dimensioned according to the extracted flow rate and the estimated mean velocity in the main duct to approach near-isokinetic sampling conditions and reduce size-dependent sampling bias. This configuration combines high-flow particle extraction with low-flow, high-resolution measurement techniques.

Temperature within the duct is continuously monitored using a thermocouple, while a differential pressure gauge measures pressure drop across selected sections of the sampling line, ensuring flow stability and supporting the interpretation of thermodynamic effects that may influence particle formation processes. The corresponding flow scheme and the experimental setup are shown in Figure 8, Figure 9 and Figure 10, respectively.

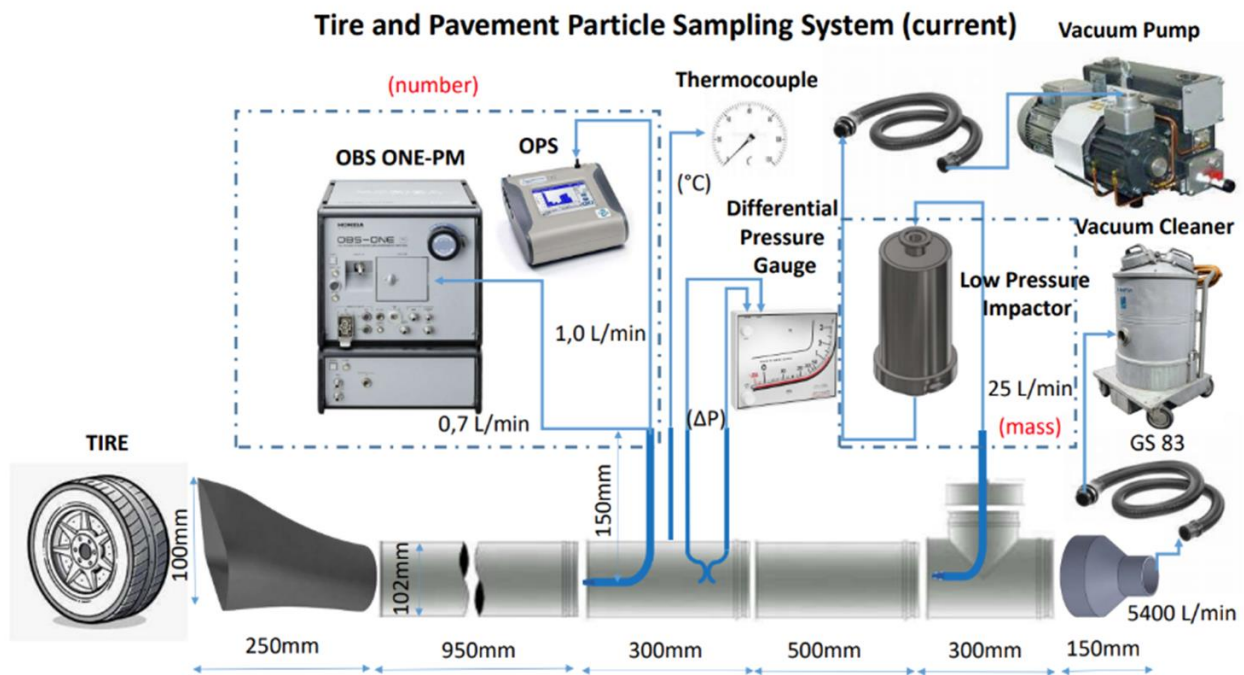


Figure 10. Flow scheme and experimental setup for particle sampling during tyre-pavement interaction



### D3.3. Properties and design of road pavements with focus on non-exhaust particle emissions

To the best of the authors' knowledge, few experimental approaches allow such a controlled and cost-effective comparison of the influence of different pavement materials on particle emissions generated at the tyre-pavement interface under repeatable laboratory conditions. Although the present setup does not fully reproduce real tyre/pavement interaction on public roads, it provides a practical platform for comparative assessment. The measured aerosol should not be interpreted as being exclusively composed of pavement-derived particles, but rather as the result of the tyre-pavement contact system. Therefore, the generated particles may include tyre wear particles, pavement wear particles, mixed tyre-pavement debris and, particularly, in the ultrafine range, particles formed through thermal volatilisation and subsequent condensation processes as the tyre/contact temperature increases. In this context, the methodology is intended to evaluate how different pavement materials influence particle generation and size distribution under controlled load, speed and tyre conditions, rather than to isolate pavement particles or reproduce absolute real-world emission factors.

The integration of the mechanical loading system with the sampling line provides a comprehensive experimental platform. The loading assembly ensures control and quantification of the normal force applied to the tyre, while the sampling system enables the capture and simultaneous characterization of particle number, size distribution, and mass under controlled and reproducible conditions.

In addition to the system description, a fixed testing protocol was followed for all experiments to ensure repeatability and to distinguish background aerosol levels from particles generated by tyre/pavement interaction. Each test was carried out on a chassis dynamometer at a constant wheel speed of approximately  $8 \text{ km h}^{-1}$ .

Before applying any contact force, a 5 min background sampling period was recorded with the vehicle at rest and the pavement block not in contact with the tyre. This stage was used to characterize the ambient and residual particle levels inside the sampling system. Afterwards, a second 5 min period was recorded with the wheel rotating at the target speed but still without contact between the tyre and the pavement specimen. This step allows the separation of particle contributions associated with wheel rotation and air entrainment from those generated by friction.

Following these preliminary stages, the pavement block was advanced toward the tyre, and a target normal load of approximately 125 N was applied through the mechanically actuated loading system, corresponding to a load-cell output signal of 1.77 mV, equivalent to 12.75 kg. The applied load was continuously monitored by the in-line load cell and adjusted when necessary to maintain stable contact conditions throughout the test. Under these conditions, particle measurements were recorded for 1 h during controlled tyre-pavement friction. Throughout the test, both the applied load and the tyre tread temperature were continuously monitored, as tyre temperature may influence particle generation mechanisms and emission rates.

Each tyre-pavement combination was tested in triplicate, maintaining the same wheel speed and target contact load in all repeated tests. Between consecutive tests, the tyre surface was cleaned using compressed air and manual cleaning procedures, and the system was allowed to cool down until the tyre returned to ambient temperature (approximately  $22 \text{ }^{\circ}\text{C}$ ).



### D3.3. Properties and design of road pavements with focus on non-exhaust particle emissions

The same tyre model was used throughout the experimental campaign, namely a Yokohama 225/50R17 98W tyre (tread wear code: 300). However, to avoid cumulative wear effects between pavement materials, a new tyre was installed whenever a new pavement sample was tested.

For each pavement sample, the specimen was weighed before each friction test and rotated by 180° after every run to reduce spatial variability in wear patterns. A total of nine friction tests were performed per pavement sample, corresponding to 9 h of accumulated use for each material. In addition, the tyre was weighed before the first test and again after completion of the full testing sequence, enabling an overall assessment of tyre mass loss during the campaign.

## 3.2 Coordination between CHM, VTI, CIEMAT, CTCON, US

The development of this task has relied on continuous coordination among CHM (as task leader), VTI, CIEMAT, CTCON and the US in order to ensure that a common and coherent approach to the technical activities have been carried out. To this end, all partners have maintained regular communication throughout these months by means of technical meeting and follow-up exchanges, which have allowed to review task progress, discuss ongoing developments and address the main methodological aspects arising at the different stages of the task.

This coordination process has played a key role in sharing the progress achieved by each partner and in jointly discussing the technical approach adopted within the task. In particular, it has enabled the alignment of methodological criteria, the exchange of preliminary observations and the consolidation of a common framework for the implementation of the experimental work and the interpretation of the results obtained. This has been especially relevant given the interdisciplinary nature of the task and the need to integrate different technical perspectives related to pavement design, testing methodologies and non-exhaust emissions associated with tyre–pavement interaction.

Overall, the coordination established among the partners has contributed to ensuring consistency between the different activities carried out within the task, while also reinforcing the robustness of the methodological approach finally adopted. Beyond the exchange of information, this collaborative process has supported joint decision-making and has facilitated the effective advancement of the work towards the objectives defined for this part of the study.

## 4. Materials

### 4.1 Aggregates

#### 4.1.1. Description of aggregate types

Aggregates play a major role in the performance of asphalt mixture, particularly in applications subjected to demanding traffic conditions, where their mechanical properties directly influence durability and surface behaviour. In this context, the selection of the aggregates of NEEVE project has been carried out considering both their expected performance and their representativeness within the framework of asphalt production in the Southeast of Spain.

In line with these criteria, a set of coarse aggregates with different mineralogical characteristics have been selected to assess their influence on the performance of the asphalt mixtures designed in Chapter 5. Specifically, two porphyritic aggregates (fractions 6/12 and 5/11) and one limestone aggregate (fraction 6/12) have been considered for the experimental programme.

The selection of these materials responds to the need to compare aggregates with markedly different mineralogical origin and mechanical behaviour. Porphyritic aggregates are typically associated with high resistance to fragmentation and polishing, making them particularly suitable for wearing courses subjected to heavy traffic, where the preservation of surface texture and skid resistance is critical. In contrast, limestone aggregates, although widely available and commonly used in conventional road applications, generally exhibit lower resistance to polishing and mechanical degradation over time.

Firstly, the porphyritic aggregate with fraction 6/12 has been analysed. The particle size distribution of this material is presented in Figure 11, where the grading curve shows a well-defined and continuous distribution within the expected limits for this fraction, indicating its suitability for use in asphalt mixtures requiring a stable coarse aggregate skeleton.

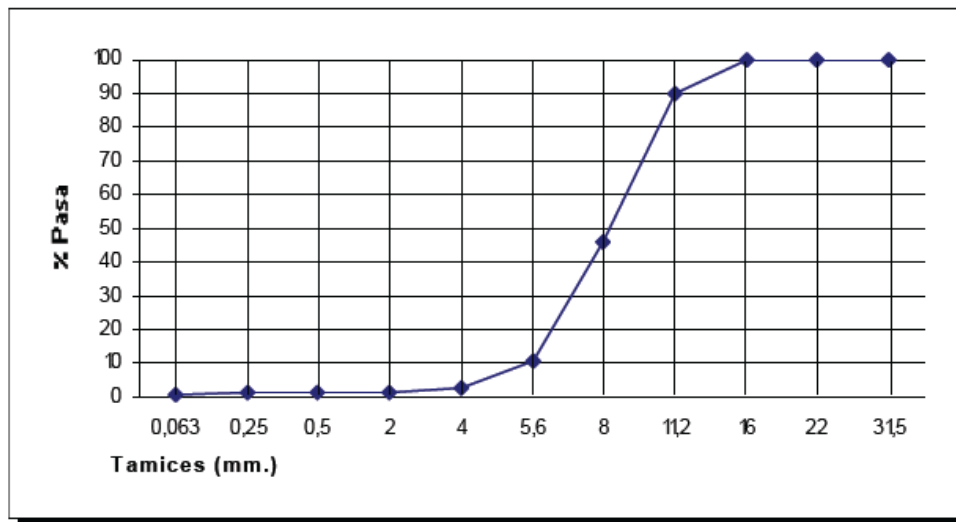


Figure 11. Particle size distribution of the 6/12 porphyry aggregate fraction

### D3.3. Properties and design of road pavements with focus on non-exhaust particle emissions

The detailed sieve analysis is presented in in Table 1, showing the particle size distribution of this aggregate fraction. These results confirm the adequacy of the material in terms of grading and its compliance with the specified particle size range.

Table 1. Aggregate sieve analysis (6/12 porphyry fraction)

Sieve Number	16	11.2	8	4	2	0.50	0.063
% Passing Aggregates	100	89.9	46.0	2.3	1.6	1.6	0.8

Secondly, the porphyritic aggregate fraction 5/11 has been analysed, showing its particle size distribution in Figure 12. This grading curve, again, shows a well-defined distribution within the expected limits for this fraction, ensuring its suitability for use in asphalt mixtures.

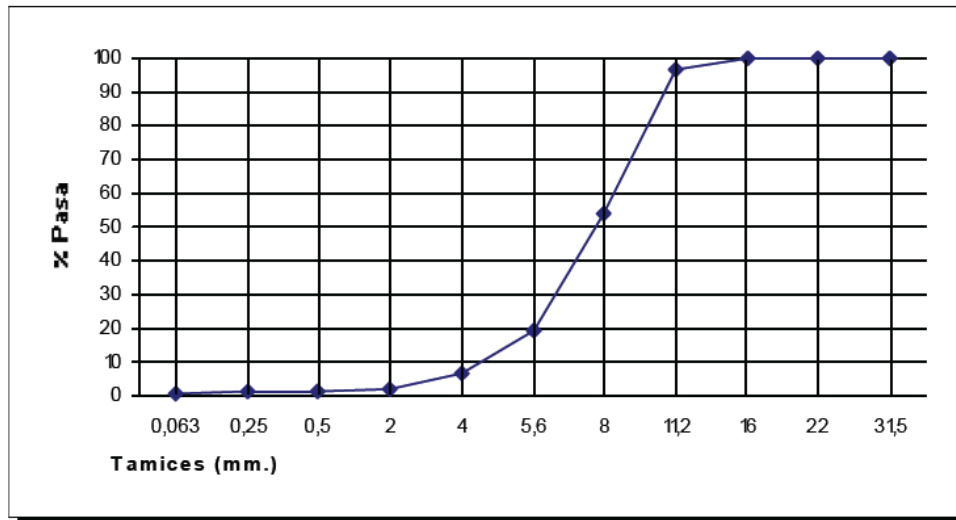


Figure 12. Particle size distribution of the 5/11 porphyry aggregate fraction

The detailed sieve analysis is presented in Table 2, showing the particle size distribution of this aggregate fraction. In comparison with the results obtained for the 6/12 fraction, the grading reflects the expected shift towards smaller particle sizes, while maintaining a continuous distribution.

Table 2. Aggregate sieve analysis (5/11 porphyry fraction)

Sieve Number	16	11.2	8	4	2	0.50	0.063
% Passing Aggregates	100	96.8	54	6.8	2.3	1.6	0.7

Finally, the limestone aggregate fraction 6/12 has been evaluated following the same procedure and its particle size distribution is presented in Figure 13. In this case, the grading curve falls within the expected limits for this fraction, showing a distribution comparable to that observed for the porphyritic aggregate 6/12.

**D3.3. Properties and design of road pavements with focus on non-exhaust particle emissions**

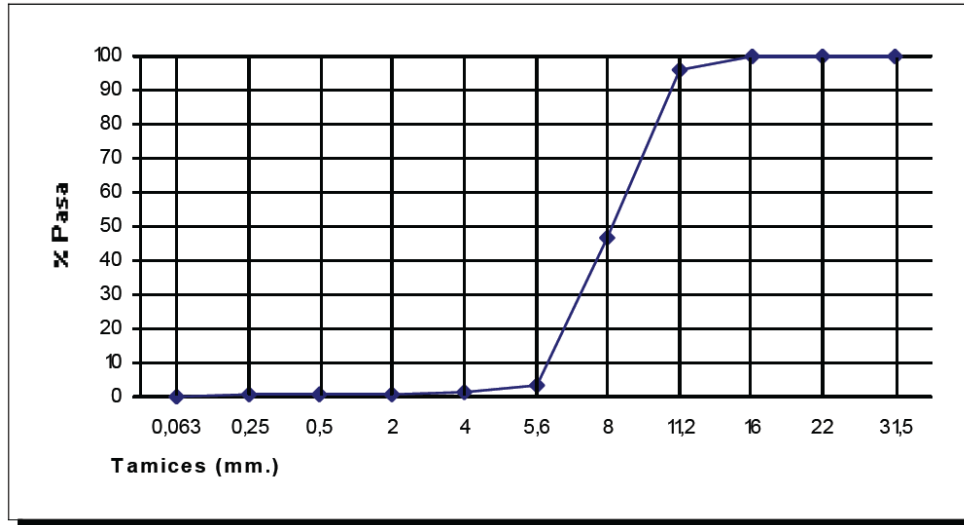


Figure 13. Particle size distribution of the 6/12 limestone aggregate fraction

Table 3.3 summarises the sieve analysis results for this aggregate fraction, providing a detailed representation of its grading. In comparison with the porphyritic aggregates, no significant differences are observed in terms of particle size distribution, confirming that all materials meet the specified grading requirements.

Table 3. Aggregate sieve analysis (6/12 limestone fraction)

Sieve Number	16	11.2	8	4	2	0.50	0.063
% Passing Aggregates	100	95.7	46.5	7.0	0.7	0.5	0.2

**4.1.2. Mechanical characterisation of aggregates**

Beyond the particle size distribution, the mechanical performance of the aggregates plays a decisive role in their suitability for use in asphalt mixtures, particularly in surface layers subjected to high traffic loads. In this context, all aggregates have been characterised in terms of resistance to fragmentation and polishing, through the Los Angeles (LA) abrasion test and the Polished Stone Value (PSV), as described in Chapter 3.

The results obtained for these aggregates are summarised in Table 4.

### D3.3. Properties and design of road pavements with focus on non-exhaust particle emissions

Table 4. Coarse aggregates mechanical characterisation

Aggregate Type	6/12 Porphyry	5/11 Porphyry	6/12 Limestone
PSV	52.3	56	45
LA (%)	12	11	24

As shown in the previous table, the porphyritic aggregates (both 6/12 and 5/11 fractions) exhibit favourable mechanical properties, with LA and PSV values consistent with the requirements for high-performance asphalt mixtures used in high traffic conditions. In contrast, the limestone aggregate (6/12) presents lower resistance to fragmentation and reduced polishing resistance, as reflected by its higher LA coefficient and lower PSV values.

According to the Spanish specifications (PG-3) for wearing courses subjected to high traffic intensity, aggregates are required to meet specific mechanical performance limits, typically defined by a Los Angeles coefficient of  $LA \leq 20-25$  and a Polished Stone Value (PSV)  $\geq 50$ , depending on the application category. In this context, the limestone aggregate does not comply with these requirements and has therefore been considered unsuitable for this application and excluded from the subsequent stages of the study.

#### 4.1.3. Chemical and mineralogical characterisation (XRD)

The mineralogical characterisation of the selected porphyritic aggregates was carried out by means of X-ray diffraction (XRD) analysis, in order to identify their main crystalline phases and to support the interpretation of their mechanical behaviour.

The analysis was performed on representative samples of the porphyritic aggregates used in the study. Prior to testing, the material was properly prepared through drying and subsequent crushing and milling, in order to obtain a fine and homogeneous powder suitable for XRD analysis. This preparation ensures an appropriate particle size and a random orientation of the crystals, which is required for a reliable identification of the mineral phases.

The XRD measurements were conducted by using a Bruker D8 Discover diffractometer operating in Bragg-Brentano geometry for bulk samples and GAXRD (Glancing Angle X-Ray Diffraction) for the filters, using a 2 mm collimator.

- Radiation: Cu  $K\alpha$  ( $\lambda=1.5406 \text{ \AA}$ )
- Power: 50 kV and 1 mA
- Scan range:  $10^\circ$  to  $90^\circ$  ( $2\theta$ ) for reference samples and  $20^\circ$  to  $60^\circ$  for filters, due to technical limitations.
- GAXRD conditions: grazing incidence angle fixed at  $\omega=1^\circ$  to maximise the signal from the surface layer of dust and minimise the signal from the filter substrate.
- Step parameters:  $0.02^\circ$  with an integration time of 0.2 s per step.

### D3.3. Properties and design of road pavements with focus on non-exhaust particle emissions

The diffraction patterns obtained (see Figure 14) show that the porphyritic aggregates are predominantly composed of silicate-based minerals, mainly quartz and feldspar phases. The main peaks identified in the diffractograms are consistent with these crystalline structures, which are typically associated with high hardness and good resistance to mechanical degradation. This mineralogical composition is in line with the favourable mechanical properties previously observed, particularly in terms of resistance to fragmentation and polishing.

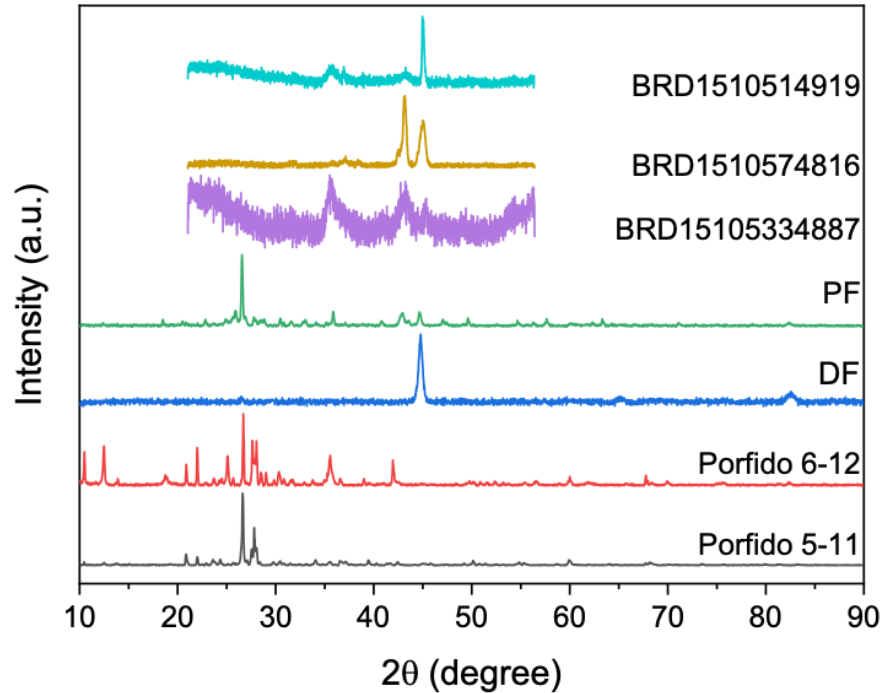


Figure 14. Diffractograms of the porphyritic fractions (5-11 and 6-12)

## 4.2 Bitumen

Within the framework of the asphalt mixture design, particular attention has been paid to the selection of the asphalt binder, given its key influence on the mechanical performance and long-term durability of the mixtures. In this context, a polymer-modified bitumen PMB 45/80-65 was chosen, as it is especially suitable for mixtures subjected to demanding service conditions, offering improved resistance to permanent deformation, better fatigue performance and increased durability.

The selection of a PMB is further justified by the specific characteristics of the mixtures investigated in the NEEVE project. On the one hand, discontinuous gradations such as SMA, PA and OSMA require a binder capable of ensuring sufficient cohesion within the mastic and adequate adhesion to the aggregate skeleton. On the other hand, the application of steel additive materials may influence the interaction between binder and aggregates, making it necessary to employ a binder with a well-balanced combination of stiffness and elasticity (Yang et al., 2025).

### D3.3. Properties and design of road pavements with focus on non-exhaust particle emissions

In order to analyse the rheological behaviour of this asphalt binder, conventional tests have been carried out (penetration, softening point and viscosity) under both unaged and short-term aged conditions. Ageing was simulated by means of the Rolling Thin Film Oven Test (RTFOT), which allows the evaluation of the binder’s susceptibility to oxidative ageing and the corresponding evolution of its properties throughout its service life. These results are presented in Table 5.

Table 5. PMB 45/80-65 rheological characterisation

Rheological Parameter	Standard UNE-EN	PMB 45/80-65	PMB 45/80-65 (RTFOT ageing)
Needle Penetration (x0.1 mm)	UNE-EN 1426	39.0	28.0
Softening Point (°C)	UNE-EN 1427	76.9	71.3
Viscosity (mPa.s)	UNE-EN 13702	536.1	659.3

Regarding the rheological response of the PMB 45/80-65, this binder exhibits high resistance to deformation at elevated temperatures while maintaining adequate flexibility at intermediate temperatures. Following RTFOT ageing, an increase in stiffness is observed, as expected due to oxidation and loss of volatile components. However, this increase remains within acceptable limits, indicating a relatively low susceptibility to short-term ageing.

This behaviour is particularly advantageous during mixing and laying operations, as well as for ensuring the long-term performance of the asphalt mixtures. Overall, the results confirm that the selected binder provides an appropriate balance between stiffness and elasticity, supporting its suitability for high-performance applications.

## 4.3 Steel Materials

As part of the alternative materials evaluated in this project, steel slag has been considered as a secondary aggregate derived from the steel production process. This material is characterised by a heterogeneous particle size distribution and a rough, irregular surface texture, as shown in Figure 15, which may enhance mechanical interlocking within the aggregate skeleton. From a compositional standpoint, steel slag typically contains oxides of calcium, iron and silicon, contributing to its high density and mechanical strength, making it a suitable candidate for use in asphalt mixtures.

### D3.3. Properties and design of road pavements with focus on non-exhaust particle emissions



Figure 15. Steel slag appearance

Considering the physical condition of the steel slag, according to the previous figure, a pre-treatment was required prior to its mechanical characterisation. In particular, this material has been subjected to a washing procedure (water plus sieving), in order to remove adhered dust, fines and other potential impurities associated with its production and handling. This treatment is essential to ensure adequate cleanliness of the material, thereby improving the binder–aggregate interaction and reducing potential variability in the performance of the asphalt mixtures. Following the pre-treatment process described above, the particle size distribution of the steel slag, presented in Table 6, reveals a predominantly fine and heterogeneous composition, with a significant proportion of particles concentrated in the smaller size fractions.

Table 6. Steel slag sieve analysis

Sieve Number	16	11.2	8	4	2	0.50	0.063
% Passing Aggregates	100	94.8	82.6	59.0	47.6	30.3	17.7

The mechanical characterisation of the steel slag was carried out by means of the Los Angeles (LA) abrasion test and the Polished Stone Value (PSV). These results are summarised as follows:

- Los Angeles Abrasion Test → 29%
- Polishing Stone Value (PSV) → 28

Overall, the mechanical performance of the steel slag can be considered inadequate. In particular, the material exhibits a relatively high fragmentation value and a low resistance to polishing, which are not compatible with the requirements for aggregates intended for asphalt mixtures, especially in high traffic conditions. Therefore, at this stage of the project and considering the materials currently available, this steel slag has been discarded for use as part of the mineral skeleton in asphalt pavements.

### D3.3. Properties and design of road pavements with focus on non-exhaust particle emissions

Nevertheless, ongoing work is focused on the identification of alternative steel slags with improved properties, aiming to obtain a material with adequate mechanical performance for its incorporation into asphalt mixtures. This includes exploring different sources, treatments and selection procedures in order to enhance the quality and consistency of the material.

In parallel with these efforts, the potential use of steel materials in asphalt mixtures has also been explored through the application of spherical steel shot (type S-170) as an additive (see Figure 16). The application of this material is supported by previous research on steel-based additives (Yang et al., 2025), which have demonstrated their effectiveness in enhancing the mechanical performance of asphalt mixtures.

From a mechanical perspective, these materials contribute to a more efficient load distribution within the mixture, promoting improved interlocking between particles and reinforcing the internal structure of the aggregate skeleton. Their high density and stiffness may also enhance the resistance of the mixture to deformation under repeated traffic loading. In addition, the incorporation of steel shot has been associated with a reduction in the susceptibility to permanent deformation and cracking, particularly in mixtures subjected to high stress levels or demanding service conditions (Patil & Hedao, 2025). This behaviour highlights their potential as a complementary additive to optimise the performance of asphalt mixtures.



Figure 16. Steel spheres additives – Appearance and relative dimensions

These spherical steel shots are characterised by its controlled particle size distribution, ranging between 0.4 and 0.8 mm, and its highly regular geometry, presenting a predominantly spherical shape with a smooth surface texture, which differentiates them from conventional angular aggregates. This material exhibits a high bulk density (approximately 4.3 g/cm<sup>3</sup>), significant mechanical strength, typical of carbon steel, and low porosity. These properties may influence the effective binder content and the interaction between the mastic and the aggregate skeleton.

Based on these characteristics and supported by previous studies on steel-based additives, the material was incorporated into the asphalt mixtures at dosages of 2.5% and 0.5% by total mixture weight. The results obtained from this incorporation are presented and discussed in Chapter 6.

## 5. Description of Asphalt Mixtures Produces

### 5.1 Laboratory production procedures

The laboratory production of asphalt mixtures has been carried out following the methodology defined in Deliverable D2.4, applying a common procedure for all the asphalt mixture hypotheses. In this context, the mixing and compaction processes were performed under controlled and repeatable conditions, in order to obtain homogeneous asphalt samples that may ensure the corresponding laboratory testing procedure.

The mixing process was carried out using a controlled two-phase procedure adapted to the characteristics of the polymer-modified binder and the aggregate gradation:

- Phase 1. The pre-heated binder was first mixed with the coarse aggregate fractions to ensure complete coating of the structural skeleton of the mixture.
- Phase 2. Fine aggregates and filler were progressively incorporated into the mixture, promoting the development of a homogeneous mastic and minimising the risk of segregation. The entire process was conducted under controlled temperature conditions to ensure adequate workability and uniform binder distribution.

Once the mixtures were prepared, compaction was carried out using two different procedures depending on the specimen type and the intended laboratory tests:

- Slab samples (UNE-EN 12697-33). Compaction was made by using a roller compactor, which enables to produce rectangular asphalt plates with dimensions of 40 × 30 cm and a thickness of 4 cm.
- Cylindrical samples (UNE-EN 12697-30). Compaction was carried out using an impact compactor, applying 50 blows per face.

Overall, the adopted laboratory production procedure allowed the preparation of consistent and representative asphalt specimens, suitable for the subsequent mechanical and functional characterisation. The combination of a controlled mixing sequence and appropriate compaction methods ensured a reliable basis for comparing the performance of the different asphalt mixture hypotheses developed within the project.

Based on this laboratory procedure, a set of asphalt mixture hypothesis were defined to evaluate how each of them would behave from a mechanical, surface and NEE perspective. In this context, three asphalt mixture configurations were considered (SMA 11, PA 11 and OSMA 11), all produced by means of porphyritic aggregates as the coarse fractions of the mixture.

As mentioned in the previous chapter, two different size fractions have been considered (5/11 and 6/12), resulting in a total of six asphalt hypothesis. Additionally, a specific experimental campaign was carried out on the OSMA mixtures, in which different dosages of metallic elements were incorporated in order to assess their influence on the mechanical behaviour and functional performance of the mixtures.

## 5.2 Reference pavement (SMA 11)

### 5.2.1. Porphyritic coarse fraction 5/11

The SMA-11 mixture produced with the 5/11 porphyritic aggregate fraction was designed following the general criteria defined in Deliverable D2.4, aiming to obtain a dense and stone-on-stone skeleton capable of providing high mechanical resistance and durability. This type of mixture is characterised by a discontinuous gradation, which promotes the formation of a stable aggregate skeleton and enhances the mechanical performance of the mixture.

The aggregate proportions selected for this mixture are summarised in Table 7. The formulation was defined to ensure an adequate balance between structural stability and workability, while maintaining the typical behaviour associated with SMA mixtures. In addition, the selected aggregate proportions were determined to comply with the requirements established in the relevant specifications.

Table 7. Aggregate gradation and composition of SMA 11 (5/11)

Aggregate	5/11P	0/4C	Filler
Dosage (%)	71.5	23.5	5.0

The particle size distribution of the mixture is presented in Table 8, where the percentage passing for each sieve size is detailed. The resulting gradation follows a discontinuous pattern, with a clear predominance of coarse particles and a reduced presence of intermediate sizes, which is characteristic of SMA mixtures.

Table 8. Aggregate sieve analysis. SMA 11 (5/11)

Sieve Number	16	11.2	8	4	2	0.50	0.063
% Passing Aggregates	100	97.7	67.1	32.7	23.6	13.7	8.7

Based on the granulometric data, the corresponding gradation curve is shown in Figure 17. As observed, the curve lies within the target envelope for SMA-11 mixtures, confirming the adequacy of the selected proportions. The shape of the curve reflects the gap-graded nature of the mixture, which is essential to achieve the desired stone-on-stone contact and to optimise the mechanical performance under traffic loading.

### D3.3. Properties and design of road pavements with focus on non-exhaust particle emissions

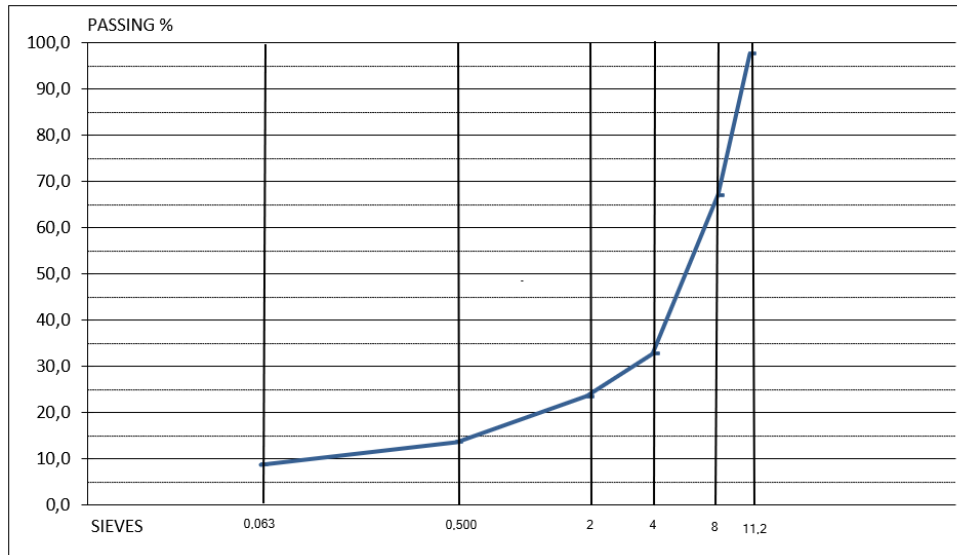


Figure 17. Grading curve as prepared for the SMA 11 (5/11)

Finally, the main volumetric properties of the mixture are summarised in Table 9, including binder content, bulk density and air voids. The selected binder content (defined in T2.4) ensures sufficient coating of the aggregate particles and contributes to the durability of the mixture, while the air void content remains within the expected range for SMA mixtures, allowing for adequate deformation capacity without compromising structural integrity.

Table 9. Volumetric characteristics SMA 11 (5/11)

<b>Bitumen content (%)</b>	5.90
<b>Void content (%)</b>	5.10
<b>Bulk density (kg/m3)</b>	2,630

#### 5.2.2. Porphyritic coarse fraction 6/12

The SMA-11 mixture produced with the 6/12 porphyritic aggregate fraction has been designed to obtain a dense and stable stone-on-stone skeleton. As in the previous case, the mixture is characterised by a discontinuous gradation, ensuring an appropriate aggregate interlock and mechanical performance.

The aggregate proportions selected for this mixture are summarised in Table 10. The formulation was defined to ensure an adequate balance between structural stability and workability, while complying with the requirements established in the relevant specifications.

**D3.3. Properties and design of road pavements with focus on non-exhaust particle emissions**

**Table 10. Aggregate gradation and composition of SMA 11 (6/12)**

Aggregate	6/12P	0/4C	Filler
Dosage (%)	68.0	27.0	5.0

The particle size distribution of the mixture is presented in Table 11, where the percentage passing for each sieve size is detailed. The resulting gradation follows the typical gap-graded distribution associated with SMA mixtures, maintaining a clear predominance of coarse particles.

**Table 11. Aggregate sieve analysis. SMA 11 (6/12)**

Sieve Number	16	11.2	8	4	2	0.50	0.063
% Passing Aggregates	100	93.1	63.3	32.8	25.5	14.7	9.3

Based on the granulometric data, the corresponding gradation curve is shown in Figure 18. The curve lies within the target envelope for SMA-11 mixtures, confirming the suitability of the selected aggregate proportions.

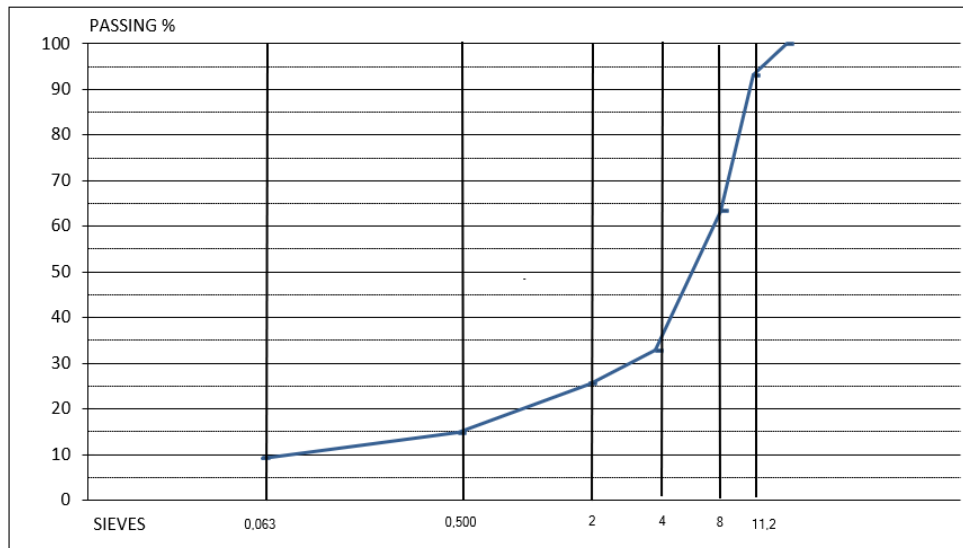


**Figure 18. Grading curve as prepared for the SMA 11 (6/12)**

Finally, the main volumetric properties of the mixture are summarised in Table 12, including binder content, bulk density and air voids.

### D3.3. Properties and design of road pavements with focus on non-exhaust particle emissions

Table 12. Volumetric characteristics SMA-11 (6/12)

<b>Bitumen content (%)</b>	5.90
<b>Void content (%)</b>	5.10
<b>Bulk density (kg/m<sup>3</sup>)</b>	2,605

## 5.3 Open graded SMA 11 (hybrid solution)

### 5.3.1. Porphyritic coarse fraction 5/11

The OSMA-11 mixture produced with the 5/11 porphyritic aggregate fraction was designed to achieve a more open internal structure compared to conventional SMA mixtures, while maintaining sufficient mechanical stability. This hybrid configuration aims to combine the structural resistance of dense mixtures with an enhanced surface functionality, particularly in terms of air voids and drainage capacity.

The aggregate dosages selected for this hypothesis are summarised in Table 13. In comparison to SMA-11 mixture, this gradation has been defined to promote a more open texture by means of increasing the proportion of coarse aggregates and reducing the fine content, in order to favour a higher void structure.

Table 13. Aggregate gradation and composition of OSMA 11 (5/11)

<b>Aggregate</b>	<b>5/11P</b>	<b>0/4C</b>	<b>Filler</b>
<b>Dosage (%)</b>	78.5	17.5	4.0

Additionally, the particle size distribution of this asphalt mixture is presented in Table 14, where the percentage passing for each sieve size is detailed. As mentioned before, the resulting gradation reflects a transition between dense and porous mixtures, with a reduced presence of intermediate and fine particles, which contributes to the development of interconnected voids.

Table 14. Aggregate sieve analysis. OSMA 11 (5/11)

<b>Sieve Number</b>	<b>16</b>	<b>11.2</b>	<b>8</b>	<b>4</b>	<b>2</b>	<b>0.50</b>	<b>0.063</b>
<b>% Passing Aggregates</b>	100	97.5	63.9	26.6	18.6	11.9	6.8

### D3.3. Properties and design of road pavements with focus on non-exhaust particle emissions

Based on this granulometric data, the corresponding gradation curve is shown in Figure 19. This curve confirms the open-graded nature of the mixture, ensuring an appropriate balance between structural integrity and functional performance.

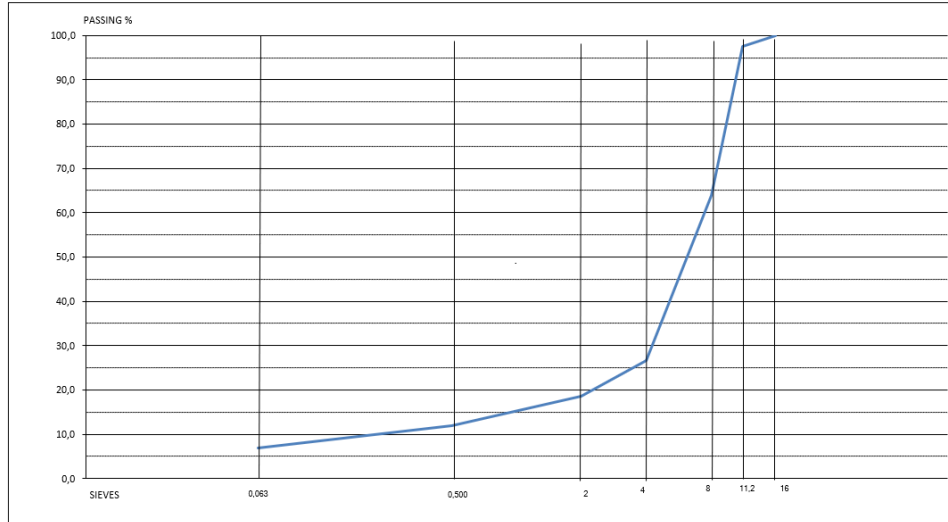


Figure 19. Grading curve as prepared for the OSMA 11 (5/11)

Finally, the main volumetric properties of the mixture are summarised in Table 15, including binder content, bulk density and air voids. As expected, the mixture exhibits a significantly higher air void content compared to SMA mixtures, which is directly related to its more open structure and is intended to enhance its functional behaviour.

Table 15. Volumetric characteristics OSMA-11 (5/11)

<b>Bitumen content (%)</b>	5.40
<b>Void content (%)</b>	12.60
<b>Bulk density (kg/m<sup>3</sup>)</b>	2,436

#### 5.3.2. Porphyritic coarse fraction 6/12

The OSMA-11 mixture produced with the 6/12 porphyritic aggregate fraction follows the same design approach described for the previous case, aiming to achieve an open internal structure while maintaining adequate mechanical stability. In this case, the aggregate proportions selected for this mixture are summarised in Table 16, aiming to promote an open gradation, characterised by a predominance of coarse particles and a reduced fine fraction.

### D3.3. Properties and design of road pavements with focus on non-exhaust particle emissions

Table 16. Aggregate gradation and composition of OSMA 11 (6/12)

Aggregate	6/12P	0/4C	Filler
Dosage (%)	74.0	22.0	4.0

In this context, the particle size distribution of this asphalt mixture is presented in Table 17, where the percentage passing for each sieve size is detailed. The resulting gradation follows the expected trend for this type of mixture, with limited intermediate sizes and a clear dominance of coarse aggregates.

Table 17. Aggregate sieve analysis. OSMA 11 (6/12)

Sieve Number	16	11.2	8	4	2	0.50	0.063
% Passing Aggregates	100	92.5	60.0	27.3	21.2	13.5	7.5

The gradation curve derived from the particle size distribution is presented in Figure 20. It reflects the open-graded nature of the mixture and supports the suitability of the selected proportions in achieving the intended structural and functional performance.

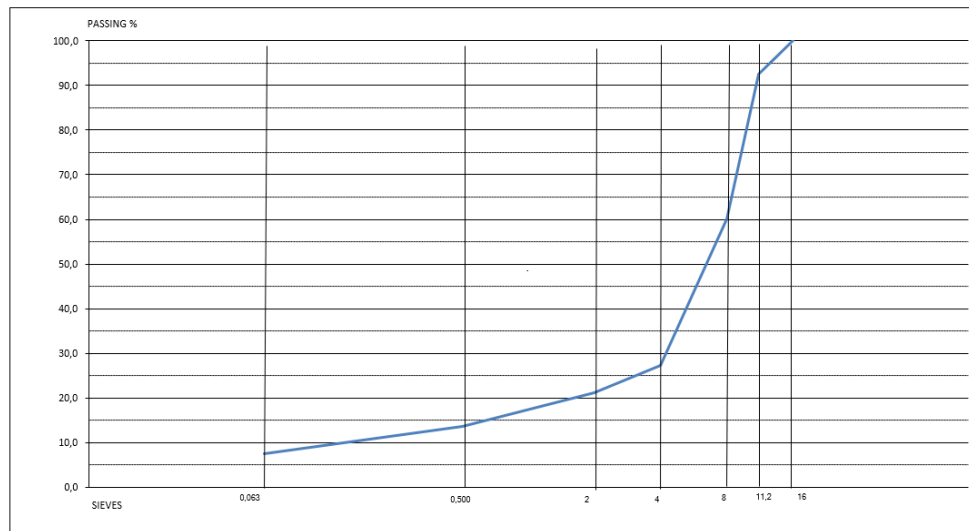


Figure 20. Grading curve as prepared for the OSMA 11 (6/12)

Finally, the main volumetric properties of the mixture are summarised in Table 18, including binder content, bulk density and air voids. In line with the design approach, the mixture presents a higher air void content than SMA mixtures, consistent with its more open structure.

### D3.3. Properties and design of road pavements with focus on non-exhaust particle emissions

Table 18. Volumetric characteristics OSMA 11 (6/12)

<b>Bitumen content (%)</b>	5.40
<b>Void content (%)</b>	12.60
<b>Bulk density (kg/m<sup>3</sup>)</b>	2,418

## 5.4 Porous asphalt pavement (PA 11)

### 5.4.1. Porphyritic coarse fraction 5/11

The PA-11 mixture produced with the 5/11 porphyritic aggregate fraction was designed to achieve a highly open structure, prioritising permeability and surface functionality. This type of mixture is characterised by a markedly discontinuous gradation, with a very limited presence of fine particles in order to maximise the interconnected air void content.

In this context, as shown in Table 19, the aggregate proportions for this asphalt mixture were defined to ensure a sufficiently open mineral skeleton. This approach allows the development of a continuous void network while maintaining the minimum stability required for handling and compaction.

Table 19. Aggregate gradation and composition of PA 11 (5/11)

Aggregate	5/11P	0/4C	Filler
<b>Dosage (%)</b>	84.5	13.0	2.5

Based on this aggregate gradation, the particle size distribution of this mixture is presented in Table 20, where the percentage passing for each sieve size is detailed. The resulting gradation shows a clear absence of intermediate and fine fractions, which is essential for promoting high permeability and effective drainage.

Table 20. Aggregate sieve analysis. PA 11 (5/11)

Sieve Number	16	11.2	8	4	2	0.50	0.063
<b>% Passing Aggregates</b>	100	97.3	61.1	20.9	13.8	8.0	4.9

In this context, the corresponding gradation curve is shown in Figure 21, highlighting the pronounced open-graded nature of the mixture and confirming the adequacy of the selected proportions in achieving the intended functional performance.

### D3.3. Properties and design of road pavements with focus on non-exhaust particle emissions

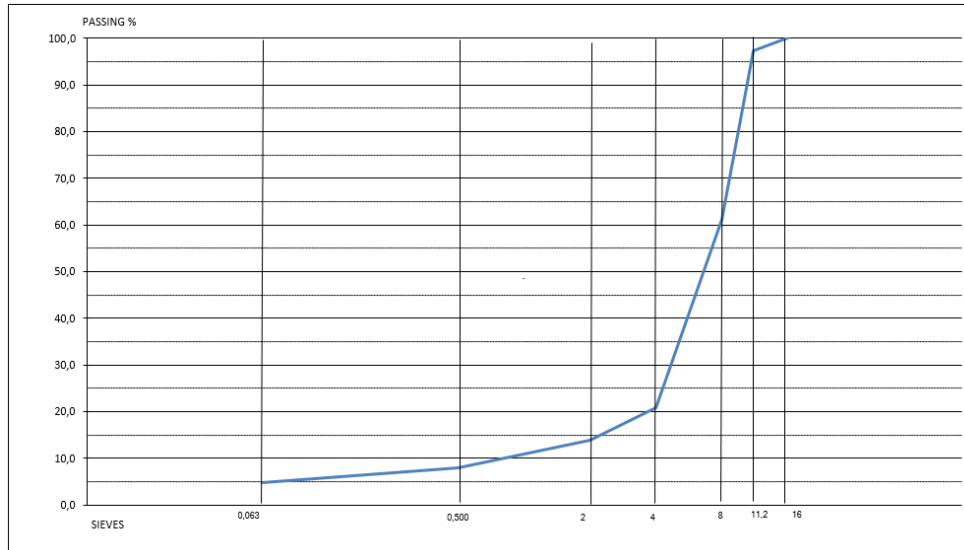


Figure 21. Grading curve as prepared for the PA 11 (5/11)

Finally, the main volumetric properties of the mixture are summarised in Table 21. As expected, the mixture presents a significantly higher air void content than both SMA and OSMA mixtures, directly associated with its open structure and its capacity to facilitate water drainage and air circulation.

Table 21. Volumetric characteristics PA 11 (5/11)

<b>Bitumen content (%)</b>	4.80
<b>Void content (%)</b>	20.10
<b>Bulk density (kg/m3)</b>	2,185

#### 5.4.2. Porphyritic coarse fraction 6/12

The PA-11 mixture produced with the 6/12 porphyritic aggregate fraction follows the same design approach described for the previous case, aiming to achieve a highly open structure with enhanced permeability and surface functionality. In this case, the aggregate proportions selected for this mixture are summarised in Table 22 and were defined to ensure the development of a stable coarse mineral skeleton with a high degree of interconnected voids, while maintaining the minimum requirements in terms of mixture integrity.

Table 22. Aggregate gradation and composition of PA 11 (6/12)

Aggregate	6/12P	0/4C	Filler
<b>Dosage (%)</b>	80.0	17.5	2.5

### D3.3. Properties and design of road pavements with focus on non-exhaust particle emissions

Additionally, the particle size distribution of the mixture is presented in Table 23, where the percentage passing for each sieve size is detailed. The resulting gradation reflects the typical characteristics of porous asphalt mixtures, with a clear dominance of coarse aggregates and a very limited fine fraction.

Table 23. Aggregate sieve analysis. PA 11 (6/12)

Sieve Number	16	11.2	8	4	2	0.50	0.063
% Passing Aggregates	100	91.9	56.8	21.3	16.4	9.4	5.6

Considering the previous table, the gradation curve derived from these data is shown in Figure 22, illustrating the open structure of the mixture and confirming the suitability of the selected proportions in achieving the intended functional behaviour.

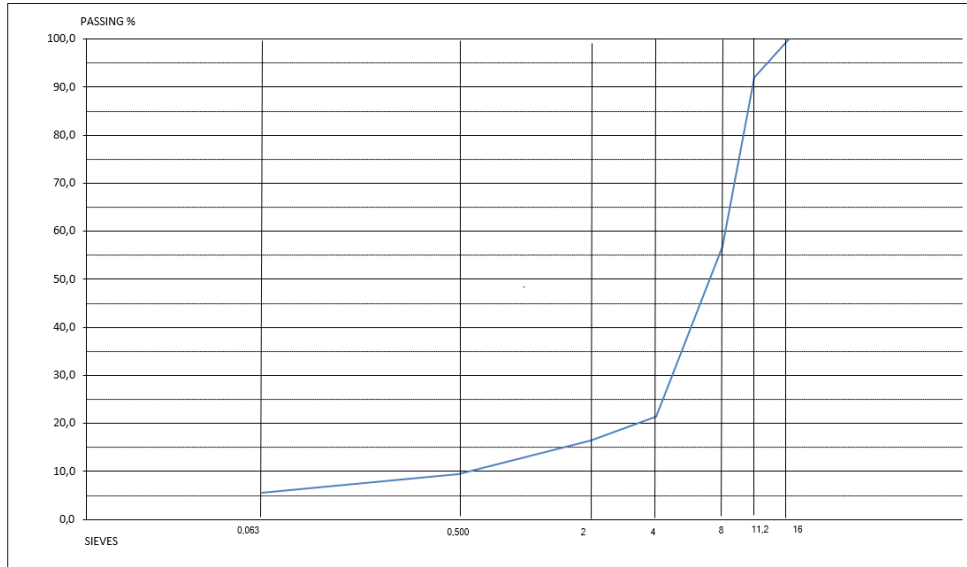


Figure 22. Grading curve as prepared for the PA 11 (6/12)

Finally, the main volumetric properties of the mixture are summarised in table 24. In line with the design objectives, the mixture exhibits a high air void content, consistent with its porous structure and its expected performance in terms of drainage and surface functionality.

Table 24. Volumetric characteristics PA 11 (6/12)

Bitumen content (%)	4.80
Void content (%)	20.10
Bulk density (kg/m <sup>3</sup> )	2,168



### D3.3. Properties and design of road pavements with focus on non-exhaust particle emissions

## 5.5 Additional pavement types evaluated

In addition to the mixtures described throughout this chapter, an alternative configuration based on the OSMA-11 mixture with 6/12 porphyritic aggregates was considered to evaluate the effect of incorporating steel particles. This particular mixture has been selected as it showed the most promising performance among the tested solutions in Deliverable D2.4 and therefore was considered the most suitable candidate for a preliminary assessment of this type of additive. In this context, spherical steel particles, previously described in Section 4 has been introduced as an additive within the mixture.

The incorporation of these particles has been evaluated at two different dosages: 0.5% and 2.5% by total mixture weight. These values were not arbitrarily selected but were based on previous studies and existing experience with similar metallic additives, as discussed in Chapter 4. This approach allows for a preliminary evaluation of the influence of the additive at different concentration levels, supporting a comparative analysis of its potential impact on the overall performance of the mixture.

## 6. Results

### 6.1 Asphalt characterisation

#### 6.1.1. Mechanical performance

The mechanical performance of the asphalt mixture has been evaluated in terms of stiffness modulus and resistance to permanent deformation. The results obtained for each different asphalt hypothesis are summarised in Table 25.

Table 25. Asphalt mechanical evaluation

Mechanical Test	SMA 11 (5/11)	SMA 11 (6/12)	OSMA 11 (5/11)	OSMA 11 (6/12)	PA 11 (5/11)	PA 11 (6/12)
Stiffness (MPa)	2264.0	2090.5	2037.5	2520.8	2190.0	1927.0
Wheel Tracking WTS (mm/10 <sup>3</sup> )	0.0241	0.0185	0.0243	0.0335	0.1030	0.1170

From a general perspective, the stiffness values show a relatively consistent range across the mixtures, with only moderate variations depending on the mixture type and the aggregate fraction used. In this regard, both SMA-11 and OSMA-11 mixtures exhibit comparable stiffness levels, indicating similar mechanical response under cyclic loading conditions. In contrast, the PA-11 mixtures tend to present lower stiffness values, especially for the 6/12 fraction, which is consistent with their more open structure and higher air void content.

Regarding the resistance to permanent deformation, the results obtained from the wheel tracking test show a consistent trend across the different mixtures. Both SMA-11 and OSMA-11 mixtures exhibit low WTS values, indicating a good resistance to rutting and a stable behaviour under repeated loading conditions, while PA-11 mixtures present significantly higher deformation rates, reflecting a lower resistance to permanent deformation.

This behaviour highlights the influence of the mixture structure on its mechanical performance, with dense and semi-open mixture (SMA and OSMA) providing a more stable aggregate skeleton compared to highly open mixtures. Additionally, it is worth noting that no significant differences are observed between the results obtained for the two-aggregate fraction (5/11 and 6/12), suggesting that both porphyritic aggregate fractions perform similarly in terms of stiffness and resistance to permanent deformation.

From a different perspective, the influence of metallic additives (spherical steel shots) on the mechanical performance of the OSMA-11 mixture was evaluated (see Table 26). The results show a clear reduction in stiffness as the steel particle content increases, indicating a progressive modification of the internal structure of the mixture. Similarly, the wheel tracking results reveal an increase in deformation rates for the modified mixtures, particularly at higher dosages, suggesting a decrease in resistance to permanent deformation.

### D3.3. Properties and design of road pavements with focus on non-exhaust particle emissions

Table 26. Influence of steel particles in the mechanical performance of OMA 11 hypothesis

Mechanical Test	OSMA 11 (BSL)	OSMA 11 (0.5% SP)	OSMA 11 (2.0% SP)
Stiffness (MPa)	2520.8	1702.5	1096
Wheel Tracking WTS (mm/10 <sup>3</sup> )	0.0335	0.074	0.079

These results indicate that, within the analysed range, the incorporation of steel particles has a negative impact on the mechanical performance of the OSMA-11 mixture. This behaviour may be associated with changes in the aggregate skeleton arrangement and the interaction between the binder and the metallic particles, which could affect the overall cohesion and load distribution capacity of the mixture.

Based on the results obtained, it can be stated that the incorporation of steel particles has a negative impact on the mechanical performance of the asphalt mixture. Therefore, within the scope of this project, the use of this additive has been discarded for the subsequent phase of the experimental programme.

#### 6.1.2. Particle loss analysis

##### Cantabro test

The resistance of the asphalt mixtures to particle loss was evaluated by means of the Cantabro test, in order to assess their susceptibility to ravelling under mechanical action. The results obtained for the different asphalt mixtures hypothesis are summarised in Table 27.

Table 27. Asphalt particle loss analysis. Cantabro test (UNE-EN 12697-17)

Asphalt Sample	Initial Mass (g)	Final mass (g)	% Loss
SMA 11 (5/11)	1310	1254	<b>4.27</b>
SMA 11 (6/12)	1319	1280	<b>2.96</b>
OSMA 11 (5/11)	1216	1157	<b>4.85</b>
OSMA 11 (6/12)	1216	1175	<b>3.37</b>
PA 11 (5/11)	1105	944	<b>14.57</b>
PA 11 (6/12)	1108	992	<b>10.47</b>

### D3.3. Properties and design of road pavements with focus on non-exhaust particle emissions

All things considered, the main findings from the Cantabro test can be summarised as follows:

- PA-11 mixtures exhibit significantly higher particle loss values, indicating a lower resistance to ravelling. This behaviour is consistent with their highly open structure and mechanical performance shown in the previous chapter.
- SMA-11 and OSMA-11 mixtures show comparable and very similar particle loss values, although slightly higher values are observed for the OSMA-11 mixtures. These results can be considered highly satisfactory, as the increase in the air void content of the OSMA-11 hypothesis does not lead to a significant deterioration in particle loss resistance.
- The 5/11 aggregate fraction consistently presents higher particle loss values across all the mixtures studied, confirming its lower resistance to mechanical degradation compared to the 6/12 fraction.

Based on the results obtained, the OSMA-11 mixtures, particularly those produced with the 6/12 porphyritic aggregate fraction, can be identified as the most promising solution in terms of overall performance. This mixture combines a relatively open graded structure with a satisfactory resistance to particle loss (similar to the one observed with the SMA-11).

Additionally, Table 28 presents the main results obtained for the OSMA-11 mixtures with spherical steel shots (based on Chapter 5.5). These results show a clear increase in the particle loss for the mixtures incorporating steel particles, which confirms that the additional of this spherical steel shots negatively affect the cohesion of the asphalt mixture.

**Table 28. Influence of steel particles in the loss of particles for OSMA 11 hypothesis**

Asphalt Sample	Initial Mass (g)	Final mass (g)	% Loss
OSMA 11 (BSL)	1216	1175	<b>3.37</b>
OSMA 11 (0.5% SP)	1206	1098	<b>8.95</b>
OSMA 11 (2.0% SP)	1222	1126	<b>7.86</b>

### Prall tests

The Prall tests (Figure 23, Table 29) made at VTI shows that:

- For the 5/11 fraction samples, the most abrasion resistant pavement construction is the SMA, followed by OSMA and PA.
- For the 6/12 fraction samples, OSMA is still higher than the SMA, while PA is in between.

These results show that the coarser fraction (6/12) should be used to reduce abrasion and production of wear particles.

**D3.3. Properties and design of road pavements with focus on non-exhaust particle emissions**

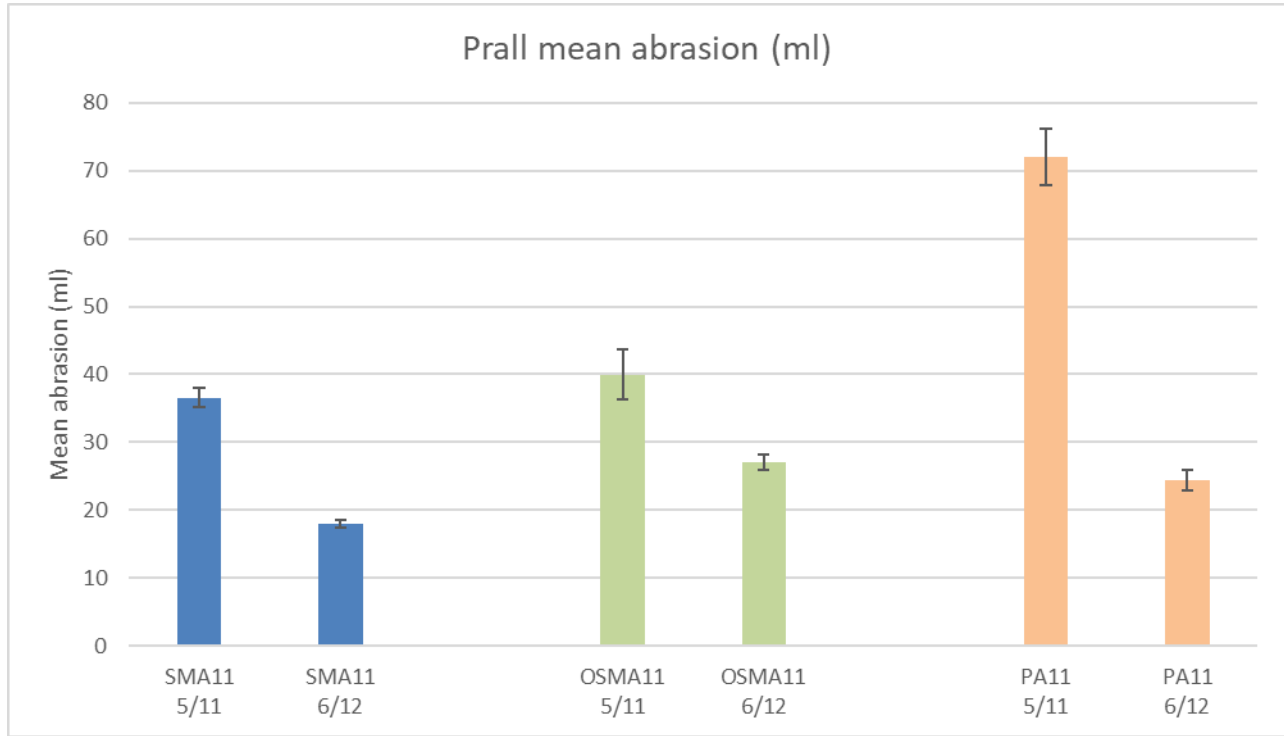


Figure 23. Results of Prall tests. Error bars are standard deviation (n=4)

Table 29. Results of Prall tests (n=4)

Sample	Mean abrasion (ml)	Std.dev. (ml)
SMA 11 (5/11)	36.58	1.38
SMA 11 (6/12)	17.94	0.58
OSMA 11 (5/11)	39.96	3.62
OSMA 11 (6/12)	27.04	1.16
PA 11 (5/11)	71.98	4.12
PA 11 (6/12)	24.39	1.50

The two particle loss test procedures confirm the influence of aggregate size within each construction type, with the PA being most sensitive, while SMA and OSMA have quite similar results (Figure 24).

**D3.3. Properties and design of road pavements with focus on non-exhaust particle emissions**

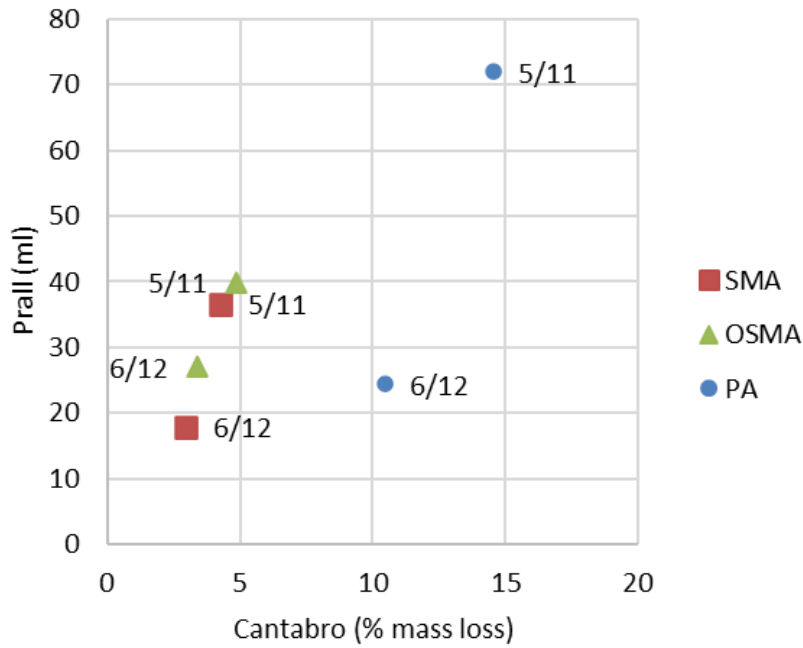


Figure 24. Prall results plotted to Cantabro results for the six samples.

**6.1.3. Texture analysis**

The surface macrotexture of the asphalt mixtures was evaluated using the volumetric patch technique, with the results obtained for the different asphalt mixtures summarised in Table 30. From a general perspective, these results clearly reflect the influence of the mixture design on the surface characteristics, showing a progressive increase in macrotexture values as the internal structure becomes more open.

Table 30. Pavement surface macrotexture analysis. Volumetric patch technique (UNE-EN 13036-1)

Asphalt Sample	Value1 (mm)	Value 2 (mm)	Mean Value (mm)	MTD/mm
SMA 11 (5/11)	215	210	213	0.7
SMA 11 (6/12)	215	210	213	0.7
OSMA 11 (5/11)	140	155	148	1.5
OSMA 11 (6/12)	155	165	160	1.2
PA 11 (5/11)	120	120	120	2.2
PA 11 (6/12)	105	110	108	2.7

### D3.3. Properties and design of road pavements with focus on non-exhaust particle emissions

In this context, considering the previous table, SMA-11 mixtures present the lowest macrotexture values, around 0.7 mm, which is directly associated with their dense structure and limited surface voids. OSMA-11 mixtures exhibit intermediate values, 1.2 and 1.5 mm (depending on the aggregate fraction), indicating a noticeable increase in surface texture due to their more open gradation. Finally, PA-11 mixtures show the highest macrotexture values, 2.2 and 2.7 mm, which can be attributed to their highly open structure.

In addition to macrotexture, the skid resistance of the mixtures was evaluated by means of the British pendulum test, with the results summarised in Table 31. In this sense, PA-11 exhibits the highest value, which can be attributed to the more open texture and surface roughness, resulting in greater friction at the tyre–pavement interface. In contrast, SMA-11 and OSMA-11 mixtures present similar and lower values, with OSMA-11 achieving comparable skid resistance levels despite its higher air void content and more pronounced surface texture.

Table 31. Asphalt friction analysis. Pendulum test applied 8 times at each direction (UNE-EN 13036-4)

Asphalt Sample	Measurement								FINAL
	1	2	3	4	5	6	7	8	
SMA 11 (5/11) LEFT	70	68	65	64	62	60	60	59	61
SMA 11 (5/11) RIGHT	70	67	65	63	62	62	61	60	
SMA 11 (6/12) LEFT	68	66	67	65	66	66	64	64	64
SMA 11 (6/12) RIGHT	70	70	68	67	65	64	63	63	
OSMA 11 (5/11) LEFT	68	65	61	60	59	58	58	57	58
OSMA 11 (5/11) RIGHT	66	64	62	59	59	57	56	55	
OSMA 11 (6/12) LEFT	69	67	63	61	59	57	57	56	58
OSMA 11 (6/12) RIGHT	67	65	64	63	60	59	58	58	
PA 11 (5/11) LEFT	73	72	68	70	67	66	66	66	67
PA 11 (5/11) RIGHT	73	74	70	69	70	68	67	67	

**D3.3. Properties and design of road pavements with focus on non-exhaust particle emissions**

<b>PA 11 (6/12) LEFT</b>	73	70	68	66	67	65	67	66	<b>66</b>
<b>PA 11 (6/12) RIGHT</b>	72	70	69	68	66	67	65	64	

*6.1.4. Drainage capacity*

The drainage capacity of the asphalt mixtures was evaluated in order to assess their ability to allow water flow through the surface layer. The results obtained for the different asphalt mixtures are summarised in Table 32, noting that no drainage tests were performed on SMA-11 mixtures due to their dense structure and low air void content, which prevent water infiltration.

Table 32. Asphalt drainability (UNE-EN 12697-40)

Asphalt Sample	Value 1 (s)	Value 2 (s)	Value 3 (s)	Drainage time (s)
<b>OSMA 11 (5/11)</b>	115	108	119	114
<b>OSMA 11 (6/12)</b>	126	123	121	123
<b>PA 11 (5/11)</b>	34	35	32	33
<b>PA 11 (6/12)</b>	39	33	33	35

The results obtained for the OSMA-11 and PA-11 mixtures show a clear influence of the mixture structure on drainage behaviour. PA-11 mixtures exhibit the highest drainage capacity, which is directly associated with their highly open structure and the presence of a well-connected network of voids that facilitates water flow. In comparison, OSMA-11 mixtures present intermediate values, indicating a noticeable drainage capacity as a result of their more open gradation, although without reaching the permeability levels observed in PA-11 mixtures.

These results highlight the potential of OSMA-11 mixtures as a balanced solution, providing a certain level of drainage capacity while maintaining a more stable internal structure than PA-11 mixtures. This combination of properties makes OSMA-11 particularly suitable within the framework of the NEEVE project.

### D3.3. Properties and design of road pavements with focus on non-exhaust particle emissions

## 6.2 NEE Physical Characterisation

A significant deviation from the nominal sampling conditions was identified during the experiments. The primary flow rate, which initially was approximately 5400 L/min, was later reduced to, approximately, 200 L/min. This was due to the decision to install a filter at the end of the sampling duct, thus generating a substantial pressure drop in the system. Nevertheless, the masses collected by the impactor allow for both a qualitative and quantitative comparison of the different pavements not for comparison with external studies (in quantitative way).

The results are summarized in Table 33 and Table 34, which provide complementary representations of the particle emissions generated under controlled tyre–pavement interaction. All particle sizes in the following are aerodynamic equivalent diameters. Table 33 presents the experimental mass distribution across grouped impactor stages (F1–F10), expressed as operational size fractions. These groupings reflect the discrete sampling characteristics of the cascade impactor and provide a direct, instrument-based description of particle mass distribution without assuming any particular underlying size distribution form. In addition, bulk indicators such as total collected mass, aerodynamic equivalent mass-median diameter (AMMD), and coarse-to-fine ratio are included to facilitate a first-level comparison between pavements.

In contrast, Table 34 provides a simplified lognormal size distribution representation of the same data by aggregating impactor stages into three physically meaningful modes: ultrafine (<70 nm), fine (PM<sub>2.5</sub>), and coarse (PM<sub>10-2.5</sub>). For each mode, the geometric mean diameter (GMD) and geometric standard deviation (GSD) are reported, providing a more physically interpretable representation of the dominant particle generation mechanisms. This dual approach enables the distinction between direct experimental observations and model-based interpretation of the emission processes.

$$\text{GMD} = \exp(\sum w_i \ln(d_i) / \sum w_i);$$

$$\text{GSD} = \exp(\sqrt{\sum w_i (\ln d_i - \ln(\text{GMD}))^2 / \sum w_i})$$

Being

- $d_i$  : midpoint diameter of each impactor stage
- $w_i$  : mass fraction in each stage
- GMD: geometric mean diameter
- GSD: geometric standard deviation

It should be noted that the defined ultrafine fraction does not match the conventional <100 nm definition, since no impactor stage features a cut-off diameter of that exact value. The closest one is 70 nm, which is the one chosen for our discussion.

### D3.3. Properties and design of road pavements with focus on non-exhaust particle emissions

In this context, Table 33 shows the particle mass distribution across impactor stage groupings for different pavement types. It should be noted that F1–F2, F3–F6, F7–F8 and F9–F10 represent grouped impactor stages based on nominal cut-off diameters (D50) of approximately 0.018, 0.035, 0.07, 0.53, 1.06, 2.09, 4.11 and 8.11  $\mu\text{m}$ .

These groupings are used as operational size fractions for comparison purposes and should not be interpreted as strict continuous particle size intervals, since particle collection in cascade impactors follows stage-specific collection efficiency curves.

Table 33. Particle mass distribution across impactor stage groupings for different types

Pavement	TM (mg)	F1-F2 %	F3-F6 %	F7-F8 %	F9-10 %	AMMD ( $\mu\text{m}$ )	Coarse/Fine ratio (F9-F10)/(F3-F6)
PA 11	0.207	7.73	41.88	24.15	26.24	~1.0	0.63
OSMA 11	0.160	1.25	57.50	18.75	22.50	~0.4–0.5	0.39
SMA 11	0.146	8.22	45.89	23.29	21.91	~0.5–0.6	0.48

Table 34. Lognormal representation of particle emissions by ultrafine, fine, and coarse modes based on impactor stage aggregation. The modes are defined according to the experimental impactor structure as follows: ultrafine (F1–F2), fine (F3–F6), and coarse (F7–F10). Note that F7–F8 represents an intermediate size range but is included within the coarse mode for the purpose of modal aggregation and analysis.

Pavement	Total mass (mg)	Mode	Mass fraction (%)	GMD ( $\mu\text{m}$ )	GSD	AMMD ( $\mu\text{m}$ )
PA 11 (I)	0.207	Ultrafine (F1–F2)	7.73	0.026	1.28	0.026
PA 11 (II)	0.207	Fine (F3–F6)	41.88	0.32	1.72	0.25–0.5
PA 11 (III)	0.207	Coarse (F7–F10)	50.39	3.10	1.85	2–8
OSMA 11 (I)	0.160	Ultrafine (F1–F2)	1.25	0.026	1.10	0.026
OSMA 11 (II)	0.160	Fine (F3–F6)	57.50	0.28	1.55	0.2–0.4
OSMA 11 (III)	0.160	Coarse (F7–F10)	41.25	2.85	1.70	1–4
SMA 11 (I)	0.146	Ultrafine (F1–F2)	8.22	0.026	1.32	0.026
SMA 11 (II)	0.146	Fine (F3–F6)	45.89	0.30	1.68	0.2–0.6
SMA 11 (III)	0.146	Coarse (F7–F10)	45.89	3.05	1.82	1–6

### D3.3. Properties and design of road pavements with focus on non-exhaust particle emissions

#### PA 11

The PA pavement exhibits the highest total particle mass (0.207 mg), approximately 30% higher than SMA (0.146 mg), indicating the most intense particle generation under identical experimental conditions. The size distribution is broad and strongly polydisperse, spanning ultrafine, fine, and coarse fractions. The emission profile is dominated by fine (41.88%) and the (50.39%) particles, which together account for more than 90% of the total mass. The ultrafine fraction contributes 7.73%, indicating a secondary but non-negligible role of high-energy fragmentation processes.

A pronounced maximum is observed at 8.11  $\mu\text{m}$  (17.9%), confirming a strong contribution of mechanically generated coarse particles associated with aggregate detachment. The median diameter (D50) is approximately 1  $\mu\text{m}$ , although the extended coarse tail indicates a highly asymmetric distribution.

Visual analysis of the pavement surface after testing (Figure 25), shows a relatively open texture with visible aggregate exposure and voids. This qualitative observation is used to describe surface morphology, although it should not be interpreted as direct evidence supporting the measured particle emissions. This texture promotes both particle generation and detachment, but also favours partial retention of tyre-derived material within surface cavities before potential re-entrainment. Overall, PA shows a particle emission pattern consistent with intense mechanical wear processes.



Figure 25. Visual appearance of PA 11 mixture, left) after 3 hours of testing testing, middle) after 6 hours of testing and, right) after 9 hours of testing

#### OSMA 11

The OSMA pavement shows a lower total particle mass (0.160 mg), corresponding to a 23% reduction relative to PA. The particle size distribution is clearly shifted towards smaller sizes and is strongly dominated by the fine fraction.

Fine particles represent 57.50% of the total mass, while ultrafine particles account for only 1.25%, the lowest among the tested pavements. The coarse fraction (F7–F10) is reduced to 41.25%, indicating a lower contribution of aggregate fragmentation-related processes compared to PA. Within this fraction, F7–F8 and F9–F10 contribute 18.75% and 22.50%, respectively

### D3.3. Properties and design of road pavements with focus on non-exhaust particle emissions

This shift is reflected in the median diameter ( $\sim 0.4\text{--}0.5\ \mu\text{m}$ ), which is significantly lower than that of PA, confirming a stronger contribution of submicron particles associated with tyre wear processes.

Visual observation of the specimen (Figure 26) shows a more compact surface structure compared to PA, with reduced void connectivity and suggests adhesion and local accumulation of tyre-derived wear debris on the pavement surface under laboratory conditions.

Overall, OSMA promotes a more stable tyre–pavement interaction, where particle emissions are primarily governed by tyre wear rather than pavement fragmentation.



Figure 26. Visual appearance of OSMA 11 mixture. Top) Before testing, Bottom) after testing

### D3.3. Properties and design of road pavements with focus on non-exhaust particle emissions

#### SMA 11

The SMA pavement presents the lowest total particle mass (0.146 mg) but in the same order of magnitude than OSMA, corresponding to reductions of approximately 30% and 9% relative to PA and OSMA, respectively. The size distribution is more balanced compared to the other pavements.

Fine particles account for 45.89% of the total mass, while coarse particles contribute 21.91%, resulting in no clearly dominant mode. The ultrafine fraction (8.22%) is comparable to PA, indicating that high-energy processes remain present despite the lower overall emission intensity.

The median diameter lies in the range of 0.5–0.6  $\mu\text{m}$ , reflecting a mixed but fine-influenced distribution. Unlike OSMA, SMA does not show a strong shift towards submicron dominance, but rather a more even partitioning between modes.

Morphologically, SMA exhibits the most compact and closed surface structure, consistent with reduced aggregate detachment (see Figure 27). However, as observed in PA and OSMA, some tyre-derived material appears to remain as adhered and locally accumulated on the surface under laboratory conditions.

Overall, SMA represents a mixed emission regime with reduced total emissions but no single dominant generation mechanism.





Figure 27. Visual appearance of SMA 11 mixture (Top) before testing, (bottom) after testing

## Global Comparison and discussion

A comparative analysis across pavement types revealed a general decrease in total particle mass from PA (0.207 mg) to OSMA (0.160 mg) and SMA (0.146 mg). All three materials exhibited broad, polydisperse size distributions spanning ultrafine, fine, and coarse fractions - a characteristic feature of tyre-road wear particles consistently reported in the literature (De Oliveira et al., 2024; Muresan et al., 2025; Grigoratos and Martini, 2014).

PA showed the highest coarse particle contribution (26.24% F9-F10), characteristic of road surface abrasion generating PM<sub>10-2.5</sub> mineral particles (Kupiainen et al., 2005; Thorpe & Harrison, 2008), whereas OSMA exhibited fine-dominated distributions (57.50% F3-F6) typical of tyre wear with maximum emissions in the submicron range (Thorpe & Harrison, 2008; Muresan et al., 2025). SMA presented a more balanced profile with comparable fine (45.89%) and coarse (21.91%) fractions, reflecting mixed wear regimes.

Despite these modal differences, OSMA and SMA showed comparable distribution patterns, with OSMA exhibiting reduced overall emission intensity relative to PA. Notably, OSMA produced the lowest ultrafine fraction (1.25% F1-F2, 18-35 nm) compared to PA (7.73%) and SMA (8.22%). Proposed formation theories for these nanoparticles may include homogeneous nucleation of tyre-derived semivolatiles under frictional heating and nano-scale cohesive rubber fragments, with compact surfaces potentially suppressing these processes through precursor retention. However, these mechanisms remain speculative in the absence of direct evidence in this study.



## 7. Risks, Limitations and Lessons Learned

The main limitation of this NEE characterization is not related to the internal consistency of the measurements, but to the representativeness of the experimental system with respect to real-world tyre–road interaction. The current configuration does not fully reproduce actual on-road aerodynamic conditions or traffic-induced dispersion processes, which limits the direct derivation of absolute emission factors. Therefore, the results should be interpreted as relative indicators of particle generation potential rather than as absolute emission factors.

Although the sampling system experienced a deviation in the global airflow conditions due to equipment constraints, the cascade impactor operated under a controlled and constant flow rate (25 L/min) for all experiments. This ensures that the size-resolved distributions remain internally consistent and comparable across pavement types. The impactor is capable of capturing particles down to approximately 18 nm; therefore, ultrafine and fine fractions are well resolved within the lower size range of the instrument.

A further limitation is related to the reduced efficiency in capturing the largest coarse particles generated by pavement abrasion, which may not be fully transported through the sampling system and are therefore partially excluded from the size-resolved measurements. As a result, complementary gravimetric analysis of pavement mass loss was required to support the interpretation of coarse particle generation.

That hybrid experimental setups combining controlled mechanical loading with high-flow aerosol sampling enable reproducible comparisons between pavement types under identical conditions, although deviations in the primary flow rate limit absolute quantification. Relative differences in total emissions (PA>OSMA>SMA) and distinct particle size distributions indicate that surface texture governs the dominant emission mechanism: aggregate fragmentation in porous surfaces versus cohesive tyre wear in compact surfaces.

OSMA appears to act as an effective reducer of the ultrafine particle fraction, minimising emissions in the lowest measured size range (1.25% vs 7.7–8.2%), which may suggest reduced generation of nano-scale debris or enhanced retention of volatile precursors. Rigorous experimental protocols (wheel rotation, triplicate tests, tyre cleaning, and controlled cooling periods) are essential to minimise spatial and temporal variability and ensure reproducibility.

## 8. Conclusions

This deliverable has provided a comprehensive assessment of the selected asphalt mixtures (SMA-11, PA-11 and OSMA-11), considering their mechanical performance, functional behaviour and their influence on non-exhaust emissions (NEE), in line with the methodological framework defined in Deliverable D2.4. The work carried out has enabled a deeper understanding of the relationship between pavement design parameters and particle generation mechanisms associated with tyre–pavement interaction.

In particular, the results obtained from the particle characterisation and quantification activities performed by CIEMAT confirm the strong influence of mixture structure on both emission levels and particle size distribution. These findings can be summarised as follows:

- PA 11 mixtures exhibit the highest total particle emissions (0.207 mg), clearly above OSMA 11 (0.160 mg) and SMA 11 (0.146 mg), confirming a more intense particle generation under identical conditions.
- OSMA 11 mixtures show an intermediate emission level combined with a fine-dominated distribution, indicative of a more stable tyre–pavement interaction.
- SMA 11 mixtures present the lowest total emissions, although with a more balanced particle size distribution and a non-negligible contribution of fine fractions.

Beyond the emission-related results, the analysis carried out in this deliverable confirms that mixture design plays a decisive role in both functional and mechanical performance. From a materials perspective, the selection of porphyritic aggregates has proven to be appropriate for high-performance applications, ensuring a stable aggregate skeleton and improved resistance to degradation, while limestone aggregates were discarded due to their lower performance.

Similarly, the comparison between the different asphalt solutions highlights the importance of balancing structural and functional properties. PA 11 mixtures provide high drainage capacity but show a greater susceptibility to particle release due to their open structure. In contrast, SMA 11 mixtures offer a dense and mechanically stable configuration, although with limited permeability. OSMA 11 mixtures achieve a more balanced behaviour, combining adequate mechanical resistance with improved functional properties, which aligns well with the objectives of the project.

In addition, the preliminary evaluation of metallic additives has not yielded satisfactory results, as they have shown a negative impact on mechanical performance and particle loss. Future work will therefore focus on identifying alternative slag materials with enhanced mechanical resistance for further assessment.

Based on the overall results obtained, the main conclusions of this work can be summarised as follows:

- Aggregate selection governs both mechanical performance and the dominant particle generation mechanisms.
- The structural configuration of asphalt mixtures defines their emission profile, particularly in terms of intensity and prevailing wear processes.



### **D3.3. Properties and design of road pavements with focus on non-exhaust particle emissions**

- OSMA 11 mixtures emerge as the most balanced solution within the scope of this study, combining reduced emission levels with consistent functional and mechanical performance.
- Particle emissions should be assessed considering both total mass and the underlying generation mechanisms.

In conclusion, the results obtained in this deliverable highlight the importance of adopting an integrated approach to pavement design, in which mechanical performance, functional behaviour and environmental impact are addressed simultaneously in order to develop more efficient and sustainable road solutions.



## 9. Acknowledgments

This LIFE-2023-SAP-ENV project number 101148428 (LIFE23-ENV-ES-LIFE NEEVE) is sponsored by the EUROPEAN COMMISSION Programme LIFE according to the information on the title page. It is also partly sponsored by the partners represented by the authors, in this case PAUDIRE INNOVA, VTI, HORIBA, ICER-BRAKES, RDT, CIEMAT, CTCOM, CHM, UMH and US.



## 10. References

- De Oliveira, T., et al. (2024). Realistic assessment of tire and road wear particle emissions and their influencing factors on different types of roads. *Journal of Hazardous Materials*, 465, 133301. <https://doi.org/10.1016/j.jhazmat.2023.133301>
- European Environment Agency. (2020). *Air quality in Europe — 2020 report*. Publications Office of the European Union.
- Gehrke, I., Schläfle, S., Bertling, R., Öz, M., & Gregory, K. (2023). Mitigation measures to reduce tire and road wear particles. *Science of The Total Environment*, 904, 166537.
- Grigoratos, T., & Martini, G. (2014). Non-exhaust traffic related emissions – Brake and tyre wear PM. JRC Science for Policy Report, EUR 26648 EN. European Commission. <https://publications.jrc.ec.europa.eu/repository/handle/JRC89231>
- Siebert, D., Mork, H.(2016): “Prall test to study the effect of mortar on the wear of Norwegian asphalt mixtures”, 6th Eurasphalt & Eurobitume Congress, 1-3 June 2016, Prague, Czech Republic.
- Kumar, Kundan; Scharr, Gerhard (2007): “Non-Pneumatic Bicycle Tire: Design Concepts and Virtual Product Development”. 26th Annual Meeting and Conference on Tire Science and Technology, Akron, OH, USA.
- Kupiainen, K.J., Tervahattu, H., Räisänen, M., Mäkelä, M., Aarnio, P., & Hillamo, R. (2005). Size and composition of airborne particles from pavement wear, tires, and traction sanding. *Environmental Science & Technology*, 39(3), 699-706. <https://doi.org/10.1021/es035419e>
- Larsson, Krister; Schade, Jörg (2004): “Optimizing the noise performance of a low-noise vehicle Wheel”. Paper 496 in Proc. of Inter-Noise 2004, Prague, Czech Republic.
- MIT (2022): “New lightweight material is stronger than steel”. News article by Anne Trafton from MIT (<https://news.mit.edu/2022/polymer-lightweight-material-2d-0202> )
- Muresan, B., et al. (2025). A study of the direct emission of tire wear particles on different types of roads. *Science of The Total Environment* 958, 178018. <https://doi.org/10.1016/j.scitotenv.2024.178018>
- Patil, D., & Hedao, N. (2025). Enhancing asphalt mixture properties through waste plastic and steel fiber additives: A comprehensive study. *Journal of Materials and Engineering Structures «JMES»*, 12(1), 5-19.
- Sandberg, Ulf (2020): “The airless tire: will this revolutionary concept be the tire of the future?” In *Modern Concepts in Material Science (MCMS)*, 3(3): 2020. MCMS. MS.ID.000563. <http://dx.doi.org/10.33552/MCMS.2020.03.000563>
- Su, J.H. (1989): "Design and analysis of a Composite Integral Wheel-Tire." *Tire Science and Technology (TSTCA)*, Vol. 17, No. 2, April-June 1989, pp 138-156.
- Thorpe, A., & Harrison, R.M. (2008). Sources and properties of non-exhaust particulate matter from road traffic: a review. *Science of The Total Environment*, 400(1-3), 270-282. <https://doi.org/10.1016/j.scitotenv.2008.06.007>



### D3.3. Properties and design of road pavements with focus on non-exhaust particle emissions

Yang, Q., Yin, W., Cheng, J., Li, Y., Zhou, Y., Chen, K., & Li, Y. (2025). Application of L-Shaped Zigzag Steel Fibers with Different Parameters in Asphalt Mixtures. *Fibers*, 13(6), 71.

Yurkovich, Chuck (2019): "When will airless tires, 3D printing and morphing trends make it into mass production?" Article in Tire Technology International 5 June 2019

(<https://www.tiretechnologyinternational.com/opinion/when-will-airless-tires-3d-printing-and-morphing-trends-make-it-into-mass-production.html> )